AD NUMBER

AD878030

LIMITATION CHANGES

TO:

Approved for public release; distribution is unlimited. Document partially illegible.

FROM:

Distribution authorized to U.S. Gov't. agencies and their contractors; Critical Technology; DEC 1970. Other requests shall be referred to Air Force Avionics Laboratory, TEL, Wright-Patterson AFB, OH 45433. This document contains export-controlled technical data.

AUTHORITY

afal ltr, 8 may 1974

AFAL-TR-70-249

RARE EARTH DOPED APATITE LASER MATERIALS

Principal Investigators: R.H. Hopkins (phone 412-256-7728)
N.T. Melamed (phone 412-256-3647)
Contributing Authors: T. Henningsen
G.W. Roland

Westinghouse Electric Corporation
Research Laboratories

Technical Report AFAL-TR-70-249

December 1970

Sponsored by Advanced Research Projects Agency
ARPA Order No. 1467
Program Code No. 9D10/A01467
Contract No. F33615-70-C-1051
Amount of Contract $300,000
Contract Dates 9/19/67 to 4/16/71

Air Force Avionics Laboratory
Air Force Systems Command
Wright-Patterson Air Force Base, Ohio 45433

NOTICE

When Government drawings, specifications, or other data are used for any purpose other than in connection with a definitely related Government procurement operation, the United States Government thereby incurs no responsibility nor any obligation whatsoever; and the fact that the Government may have formulated, furnished, or in any way supplied the said drawings, specifications, or other data, is not to be regarded by implication or otherwise as in any manner licensing the holder or any other person or corporation, or conveying any rights or permission to manufacture, use, or sell any patented invention that may in any way be related thereto.

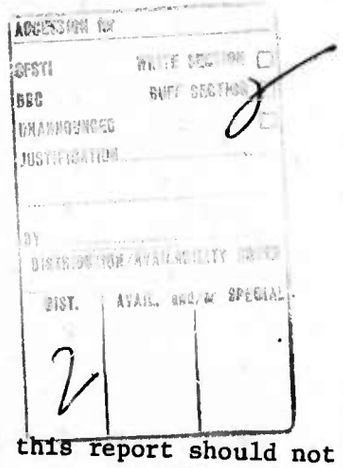

Copies of this report should not be returned unless return is required by security considerations, contractual obligations, or notice on a specific document.

RARE EARTH DOPED APATITE LASER MATERIALS

R.H. Hopkins, N.T. Melamed, T. Henningsen, et al

Westinghouse Electric Corporation

Research Laboratories

FOREWORD

This is the second semi-annual report on Contract F33615-70-C-1051 and covers work performed to evaluate rare-earth doped apatite laser materials. These studies were carried out at the Westinghouse Electric Corporation, Research Laboratories, Pittsburgh, Pa. 15235.

Mr. Richard L. Remski (TEL), Air Force Avionics Laboratory, Air Force Systems Command, Wright-Patterson AFB, Ohio is the Project Monitor for this program which is sponsored under ARPA Order Number 1467.

This report was submitted by the authors on 3 October 1970 and covers the period from 20 March 1970 to 19 September 1970. Dr. R. Mazelsky, Manager, Inorganic Preparation and Crystal Growth is Project Supervisor and Drs. N.T. Melamed and R.H. Hopkins are principal investigators. Mr. T. Henningsen and Mr. P. Buchhave have been responsible for laser testing while Dr. G.W. Roland has directed investigations of crystal chemistry.

We gratefully acknowledge the technical assistance of R. Perevuznik, A.M. Stewart, and V. Toth in various phases of the experimental work. Other contributors to this program were Dr. J.D. Feichtner, refractive index measurements, Dr. D.H. Damon and P. Piotrowski, thermal conductivity, J. Valentich, thermal expansion and M. Walker and J. Uphoff, heat capacity.

This technical report has been reviewed and is approved for publication.

Amos H. Dicke

AMOS H. DICKE
Chief, Laser Technology Branch
Electronic Technology Division

Abstract

This second semi-annual report describes the current status of the second and third phases of a program to evaluate certain members of the mineral family apatite as hosts for the active laser ion holmium.

A systematic study of the influence of growth parameters on the quality of fluorapatite (FAP) crystals doped with Ho and Cr indicates that pull rates below 2 mm/hr and a rotation rate of 80 rpm are optimum for crystal growth. For these conditions the effective distribution coefficients of Ho and Cr in FAP are 0.34 and 0.24, respectively.

The physical properties of FAP and triply-doped CaYSOAP, $CaY_4(SiO_4)_3O$, have been measured and compiled. The thermal conductivity of CaYSOAP (0.016 watts $cm^{-1}{}^{\circ}K^{-1}$ at RT), like that of FAP, is relatively low. Thermal expansion coefficients are $5.7 \times 10^{-6}\ {}^{\circ}K^{-1}$ along [0001] and 7.1×10^{-6} along $[10\bar{1}0]$ at room temperature for CaYSOAP, indicating that crystallographic anisotropy is relatively small for this property.

CaYSOAP has a threshold of 30 to 60 joules at liquid nitrogen temperature when tested in long pulse operation. Despite high scattering losses, 10 to 15% cm^{-1}, in our early crystals slope efficiencies as high as 0.61% have been measured. YAG:Ho rods with 1 to 4% cm^{-1} losses had slope efficiencies of 1.2% when tested in an identical fashion. We obtained a Q-switch output of 50 mj with 135 J input to the lamp for CaYSOAP. No saturation of the output was observed up to the maximum input energy.

YAG crystals damaged each time we attempted to Q-switch them in our laser head. The broad fluorescence linewidth ($\sim$ 250Å), lack of saturation, apparent resistance to damage and potential efficiencies of CaYSOAP suggest this material may have possible use in Q-switched applications.

TABLE OF CONTENTS

TABLE OF CONTENTS (cont'd) PAGE

LIST OF ILLUSTRATIONS

LIST OF ILLUSTRATIONS (cont'd)

LIST OF ILLUSTRATIONS (cont'd)

1. REPORT SUMMARY

The purpose of this program is to assess the merits of fluorapatite (FAP) and a silicate oxyapatite, CaYSOAP, as hosts for the active laser ion holmium. The objectives of this phase of the program were to initiate crystal growth refinement for these hosts, catalog their physical properties and begin active laser testing of crystals of each material.

We have carried out a systematic evaluation of the effect of pull and rotation rate on the crystal quality and dopant segregation of FAP:Ho,Cr. Pull rates below 2 mm/hr combined with crystal rotation of about 80 rpm enhance FAP crystal quality. Under these conditions the effective distribution coefficients of Cr and Ho in FAP are 0.24 and 0.34 respectively. The primary scattering defects in CaYSOAP crystals are second phase particles. We are evaluating the effect of melt composition on the presence of these defects.

The indices of refraction, thermal conductivity, thermal expansion, heat capacity, hardness and lattice parameter of $CaY_{2.25}Er_{1.5}Tm_{.15}Ho_{.1}(SiO_4)_3O$ crystals have been measured. CaYSOAP, like FAP, has somewhat low thermal conductivity and little crystallographic anisotropy in thermal expansion. The physical properties of FAP:Ho,Cr were determined previously and have been reported.

Long pulse laser testing of CaYSOAP:Er,Tm,Ho shows that this material has a threshold at liquid nitrogen temperature of about 30-60 joules, or about ten times that of YAG. This is in agreement with the fact that the predominant 2μ fluorescence line of Ho in CaYSOAP is about ten times broader than that of YAG. The slope efficiencies of CaYSOAP were somewhat lower than those of YAG probably due to the higher scattering losses (10-15% cm^{-1}) in these early CaYSOAP crystals compared to the losses in YAG (1-4% cm^{-1}). We expect that improvement in crystal quality of CaYSOAP will reach the slope efficiency of this material comparable to that of YAG.

We obtained a 50 mj Q-switched output from a CaYSOAP:Er,Tm,Ho rod at 135 joules was input to the lamp. No saturation in Q-switched output was observed up to the maximum input. When we attempted to Q-switch YAG rods we found that the crystals repeatedly damaged during each test. No damage was observed in the CaYSOAP rods under identical conditions. We feel the higher energy storage of CaYSOAP (due to its wide fluorescence line), its resistance to damage, and the apparent lack of saturation and potential efficiency all favor the usefulness of this material in Q-switch applications.

2. INTRODUCTION

2.1 PROGRAM OBJECTIVES AND APPROACH

This document is the second semi-annual report concerning the status of an investigation of rare-earth doped apatite laser materials. The primary objective of this program is to assess the capabilities of certain members of the apatite mineral family as hosts for the active laser ion holmium. The materials to be evaluated include fluorapatite (FAP), which has previously demonstrated laser oscillations of a two micron wavelength when doped and sensitized with Ho and Cr, respectively,[1] and one member of a new series of compounds, silicate oxyapatites (SOAP).[2]

Our approach to this investigation was first to determine the most promising silicate oxyapatite among those based on La, Gd or Y as the trivalent host constituent, then to optimize the dopant and sensitizer concentrations of this "best" host to obtain efficient Ho fluorescence. At this point our knowledge of the spectroscopic properties of FAP and SOAP became essentially equal and we then proceeded to examine those areas of interest common to both materials, including crystal growth, detailed spectroscopy and active laser testing.

To reiterate, the overall program consists of four phases:[2]

1. Choice of best SOAP host, $CaR_4(SiO_4)_3O$ where R=La, Gd, or Y, by spectroscopic analysis of polycrystalline samples prepared with and without the sensitizers Er and Tm.

2. Optimization of dopant and sensitizer composition in FAP and the chosen SOAP by spectroscopic analysis and laser testing of the initially grown crystals. Collection of physical property data for both materials and initial crystal growth refinement.

3. Final refinement of laser crystal growth combined with intensive laser testing of the grown crystals to determine their capabilities in pulsed, CW and Q-switched operation.

4. Comparison of the laser properties of the optimized apatite host with those of other current holmium host materials.

2.2 REVIEW OF PREVIOUS WORK

Phase one of the program has been completed and the results were reported in detail in the first semi-annual report on this contract.[2] As background we review the highlights of that work. CaYSOAP, $CaY_4(SiO_4)_3O$, was the most promising of the three silicate oxyapatites we examined, both from the standpoint of efficient Ho fluorescence at 2 microns and with respect to the quality of the crystals grown. Spectroscopic evaluation of sensitized polycrystalline samples indicated that the composition $CaY_{2.25}Er_{1.5}Tm_{.15}Ho_{.1}(SiO_4)_3O$ would be near optimum for laser action. The first CaYSOAP rod grown during the program, although not of the optimum composition, lased with a threshold of 30 joules at 77°K thus confirming our expectations of laser action based upon spectroscopic studies of the polycrystalline material.

We also designed and constructed a versatile low temperature laser testing facility. The apparatus is suitable for long pulse, CW, and Q-switched laser operation at temperatures between 72 and 300°K, can handle laser rods and pump lamps of various sizes, and is compatible with existing power supplies, resonator mounts, detectors and Q-switches.

3. CURRENT PROGRAM STATUS

Work during the past six months has centered upon the second and third phases of the program and has included the following: a systematic study of the growth and quality of both FAP:Ho, Cr and triply-doped CaYSOAP crystals, spectroscopic analysis of the crystals and active laser testing of both the pulled apatite crystals and specimens of commercial "ABC" YAG. We have also measured or obtained from the literature values for those physical properties of each apatite host which are most important for laser system design.

3.1 MATERIALS

3.1.1 Crystal Growth Refinement

3.1.1.1 CaYSOAP:Er, Tm, Ho

We noted before that the most common defects in triply-doped CaYSOAP crystals were second phase inclusions and that at pull rates less than about 2 mm/hr (0.08"/hr) such defects tended to be minimized.[2] During attempts to optimize growth parameters further we have discovered that these crystals may also tend to become hazy or cloudy under certain conditions. This haze is caused by the distribution of fine particles, evidently precipitates, throughout some portions of a crystal. These particles, which can be resolved with an optical microscope at 200 to 500x magnification, sometimes appear preferentially aligned along certain directions of the crystal indicating that precipitation occurs preferentially along dislocation lines as happens in FAP:Nd crystals.[3]

While the exact nature and origin of the fine second phase particles is not yet clear, we do know that exposing crystals to high temperatures for prolonged times tends to increase the incidence of the particles. For example, crystals held at temperatures near 2000°C for twelve hours were uniformly hazy while crystals cooled directly to room temperature over a two to three hour period contained very little haze.

The presence of both inclusions and precipitates in our crystals strongly suggests that the stoichiometric melt composition, $CaY_4(SiO_4)_3O$, from which crystals are grown may not be the maximum melting temperature composition for yttrium silicate oxyapatite. For this reason we have begun to study the microstructure of crystals pulled from non-stoichiometric melts. Initially melt compositions in the ternary system $CaO-Y_2O_3-SiO_2$ deviating about 2 mole % from the composition $CaY_4(SiO_4)_3O$ were chosen for study (e.g., points A, B, and C in Fig. 1). Crystals grown from these melts contained more second phase than the stoichiometric crystals hence we had apparently deviated too far in composition. We are continuing this work with melt compositions deviating only 0.5 mole % from stoichiometry.

Concurrent with these investigations several triply doped crystals have been grown for spectroscopic measurements and active laser testing (section 3.3). Subsequent to optical transmission measurements (section 3.2.2.3) several crystals were submitted for chemical analysis. From this data both absorption cross-sections and distribution coefficients can be deduced for each of the trivalent rare earth ions. Our preliminary

Curve 594889-A

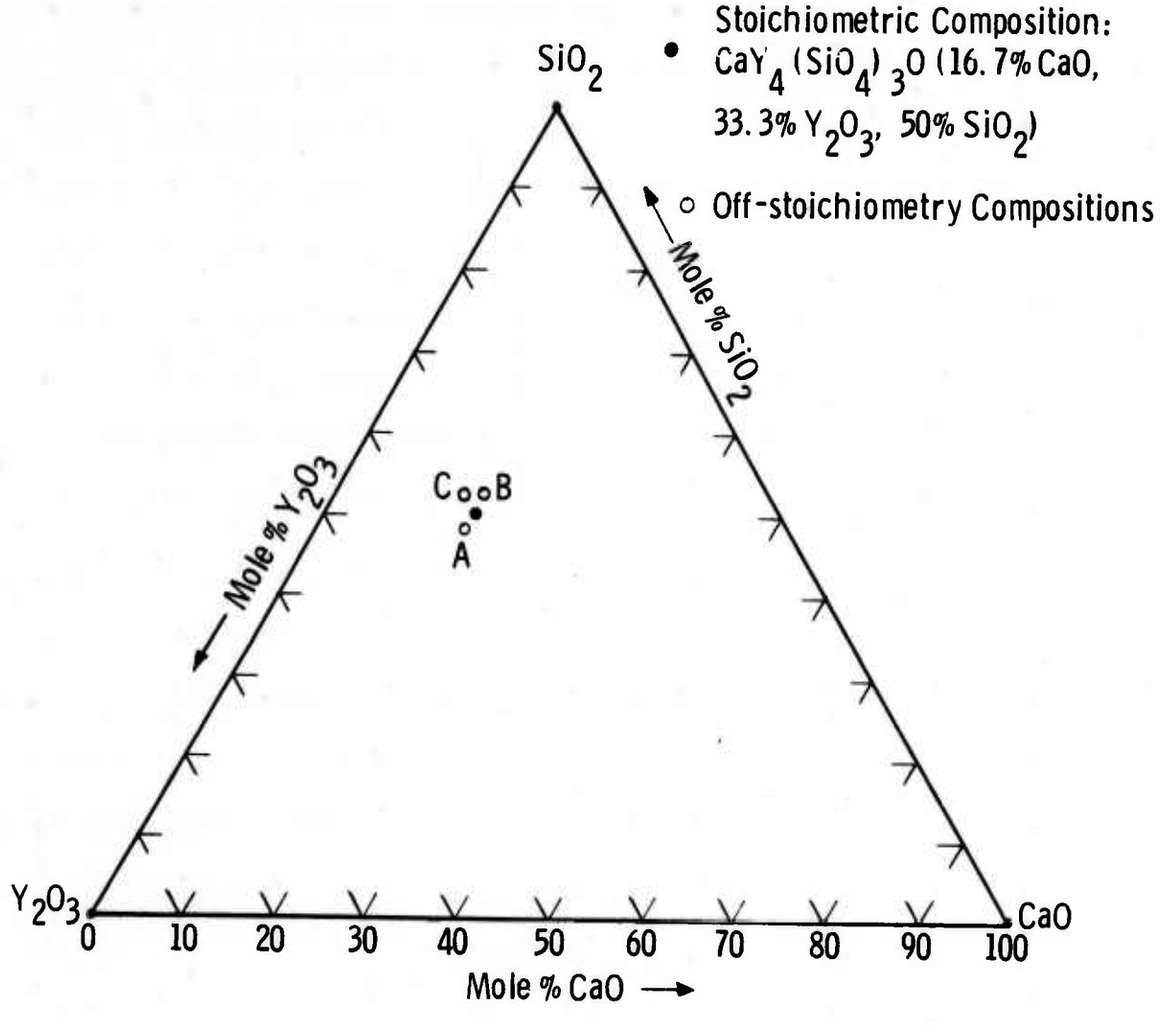

Fig. 1

results indicate that the effective distribution coefficients of Er^{+3}, Tm^{+3} and Ho^{+3} in CaYSOAP are all greater than 0.9.

3.1.1.2 FAP:Ho, Cr

We are carrying out a systematic examination of the effect of growth parameters, such as pull and rotation rate, upon the dopant segregation and crystal quality of FAP:Ho, Cr. Crystal quality was assessed by means of passive microscopic examination and active laser testing. The Ho and Cr content of crystals was determined by atomic absorption spectroscopy after calibrating the method with FAP samples having known Ho and Cr concentration.

All crystals were prepared from reactant materials and grown in the Czochralski furnace as described elsewhere.[4,7] Initially we chose pull rates in the range 1 to 10 mm/hr since this spectrum of pull rates is of greatest practical interest. Slower rates are economically undesirable while faster rates promote crystal fracture.[5] Rotation rate was varied between 0 and 150 rpm. The Ho and Cr contents in the melts from which crystals were grown lay in the range $0.10 \leq x \leq 0.15$ and $0.002 \leq y \leq 0.01$, respectively, where x and y refer to the general chemical formula $Ca_{5-x}Ho_x(PO_4)_{3-y}Cr_yF$. Previous spectroscopic analysis of polycrystalline sample had shown that compositions within these limits would optimize holmium fluorescence intensity in FAP.[1,2]

Before discussing in detail the results of our experiments it will be helpful to review briefly some aspects of solute redistribution during freezing. Generally, when a liquid containing solute (either intentionally added or accidentaly present) freezes, the resulting crystal contains less

solute than the liquid from which it froze. The excess solute rejected by the crystal builds up ahead of the solid-liquid interface forming a boundary layer. In the extreme case when the freezing rate is very small and the liquid well mixed, the boundary layer is of zero thickness, then solute redistribution is given by k_o, the equilibrium distribution coefficient. k_o is the ratio of solute concentrations in the solid and liquid at equilibrium and can be obtained from the phase diagram of the system. In most experiments, however, freezing conditions are such that a solute boundary layer is present and it is the magnitude and stability of this boundary layer which determines macro and microsegregation of impurities in a crystal.

Qualitatively, when the freezing rate, R, is high, the solute concentration of the bulk liquid, C_∞, is large, and the temperature gradient, G, in the liquid is low, then the planar crystal-liquid interface may become unstable, the boundary layer perturbed, and solute incorporated non-uniformly in the crystal (perhaps as second phase inclusions). If growth is in a stable region, increasing the growth rate or decreasing the rotation rate, w, (Czochralski pulling) increases the solute concentration of the boundary layer; this effect is reflected by a concomitant increase in the crystal solute concentration. Under these conditions solute redistribution can be characterized by an effective distribution coefficient, k_e, which is the ratio of the solute concentration in the crystal to that in the bulk liquid. k_e is thus a function of R, w, and k_e.

In our initial experiments we used Mallinkrodt Standard Luminescent Grade CaF_2 as a reactant material. All crystals pulled faster than 1.5 mm/hr

contained inclusions. By switching to single crystal CaF_2 chips we greatly improved the quality of our crystals. Evidently the SI Grade CaF_2 contained enough impurity to cause interface breakdown. Even with higher purity CaF_2 we note that crystals tend to fracture when pull rate exceeds 5 mm/hr.

For a fixed rotation rate, crystal quality improved as pull rate was decreased, although crystals for which R exceeded 2 mm/hr still contained dopant nonuniformity. In the worst cases of dopant inhomogeniety crystals failed to lase. As one might expect, raising rotation rate (> 120 rpm) permitted a higher growth rate to be sustained without interface breakdown. This benefit was offset, however, by the formation of a swirl-like appearance in the crystal. This effect has been noted in other Czochralski-grown crystals.[6] Best crystals were obtained with R=1.5 mm/hr and w=80 rpm.

The incorporation of Ho and Cr into FAP crystals followed the dependence on growth rate and rotation rate that was expected. For example, with R fixed, R=5 mm/hr. k_e^{Ho} decreased from 0.397 to 0.369 as w increased from 6 to 150 rpm. With w fixed at 80 rpm, k_e^{Ho} increased from 0.344 to 0.431 as pull rate was varied from 1.5 mm/hr to 10 mm/hr. We obtained the same value of k_e^{Ho}, within error, when crystals were singly doped or contained Ho and Cr. k_e^{Ho} did not vary with the melt Ho content for the values of C_∞^{Ho} which we used. The value of k_e^{Cr} was almost insensitive to variation in pull and rotation rate and was equal to $0.24 \pm .02$ except at the lowest pull and rotation rate employed. At R = 1.5 mm/hr and w = 6 rpm $Ke^{Cr} = 0.34$. We do not fully understand the apparent constancy of k_e^{Cr}.

3.1.2 Physical Property Measurements

3.1.2.1 CaYSOAP:Er, Tm, Ho

To complete the material characterization of CaYSOAP we have measured the indices of refraction, thermal conductivity, thermal expansion, heat capacity, lattice parameters and hardness on either single crystalline or polycrystalline samples. The sample composition for each measurement was $CaY_{2.25}Er_{1.5}Tm_{.15}Ho_{.1}(S.O_4)_3O$ corresponding to the optimum doping levels deduced from spectroscopic data.[2] All results are summarized at the end of this section in Table 1.

3.1.2.1A Indices of Refraction

Single crystals of CaYSOAP:Er, Tm, Ho were fabricated into prisms with wedge angles of about 25°. (The angle of each wedge was determined to $\pm$ 3'). The crystallographic c direction was parallel to the line of intersection of the prism faces. The indices of refraction for the ordinary (o) and extraordinary (e) rays could then be obtained by measuring the angle of deviation of light incident on the prism and applying the formula $\eta_{o,e} = \frac{\sin 1/2(A+D)}{\sin (A/2)}$, where A=prism angle and D= the angle of deviation of the incident beam. The wavelength of the incident light was varied by means of a spectrometer and we found that η_o and η_e vary between 1.79 and 1.84 over the wavelength interval 0.5 to 1.2μ, Fig. 2. The crystals are uniaxial negative with birefringence approximately 0.02. The estimated error of measurement is indicated in the figure.

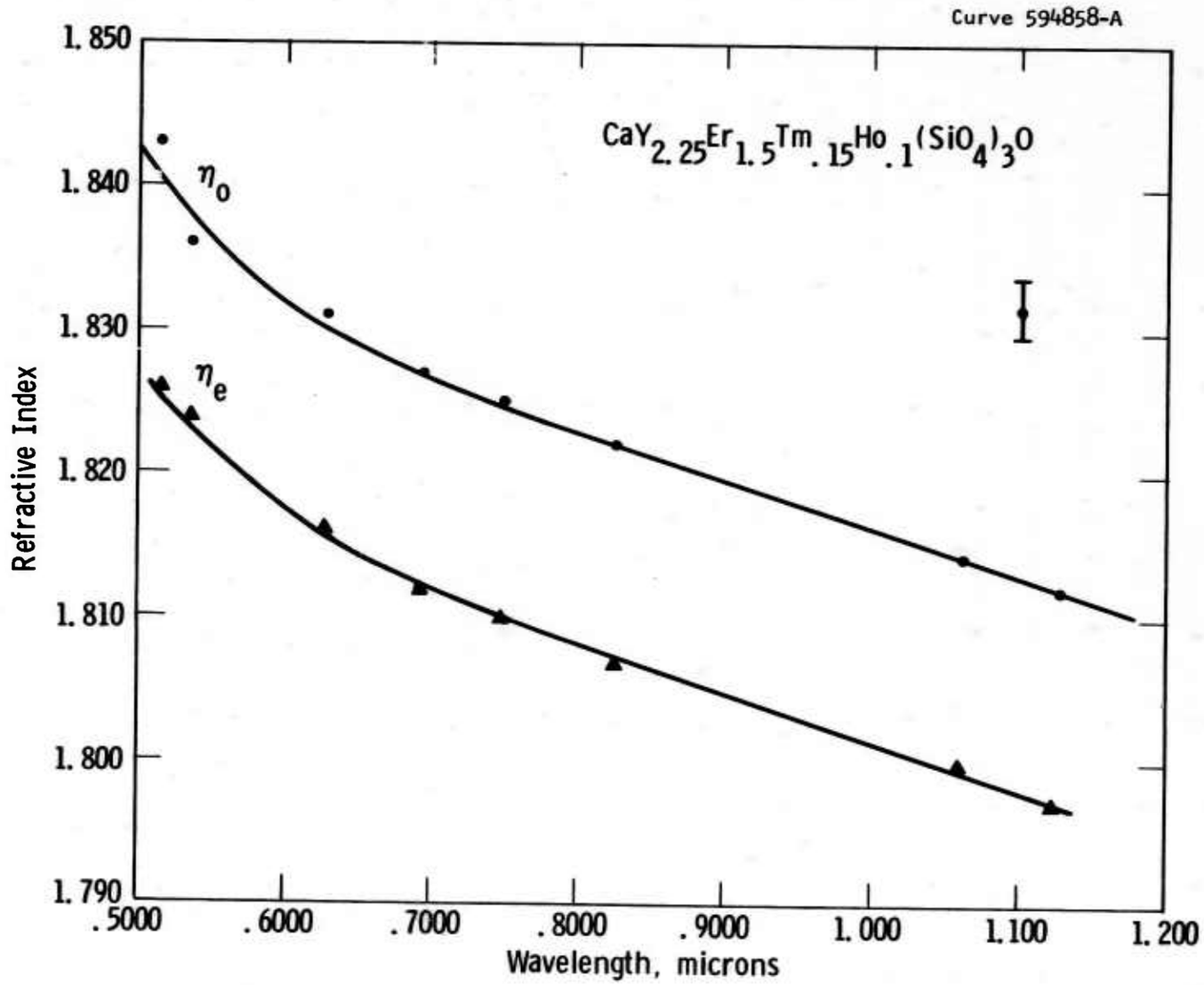
Curve 594858-A
$CaY_{2.25}Er_{1.5}Tm_{.15}Ho_{.1}(SiO_4)_3O$
η_o
η_e
Refractive Index
1.850
1.840
1.830
1.820
1.810
1.800
1.790
.5000
.6000
.7000
.8000
.9000
1.000
1.100
1.200
Wavelength, microns

Fig. 2

3.1.2.1B Thermal Conductivity

A single crystal of CaYSOAP:Er, Tm, Ho grown in the [0001], c, direction was fabricated into a right circular cylinder 1.0 cm high x 0.6 cm diameter. The thermal conductivity of this crystal was measured by the stationary heat flow method previously used to study FAP:Nd (Appendix I). Heat flow was along the c direction.

The variation in thermal conductivity, K, with temperature is shown in Fig. 3. The conductivity is relatively low, about 0.016 watts $cm^{-1}{}^{\circ}K^{-1}$ at room temperature, and only slightly temperature dependent, as in the case of FAP.[7] Conductivity of CaYSOAP apparently increases monotonically with temperature contrary to FAP for which conductivity is greatest at high and low temperature and least around 300°K.

3.1.2.1C Thermal Expansion

The thermal expansion of two $CaY_{2.25}Er_{1.5}Tm_{.15}Ho_{.1}(S.O_4)_3O$ single crystals was measured as a function of temperature by means of a quartz tube dilatometer. The samples were right circular cylinders about 2.54 cm long x 0.6 cm diameter fabricated from crystals grown in the [0001] and $[10\bar{1}0]$ directions, respectively. All measurements were made in air and were carried out over the temperature interval 77 to 1173°K. From this expansion data, Fig. 4, we can deduce that the expansion coefficients for CaYSOAP:Er, Tm, Ho are about $5.7 \times 10^{-6}{}^{\circ}K^{-1}$ and $7.1 \times 10^{-6}{}^{\circ}K^{-1}$ at room temperature for the [0001] and $[10\bar{1}0]$ directions, respectively. As in the case of FAP (Table 1) there is no marked crystal anisotropy in the expansion coefficients of CaYSOAP.

Curve 594890-A

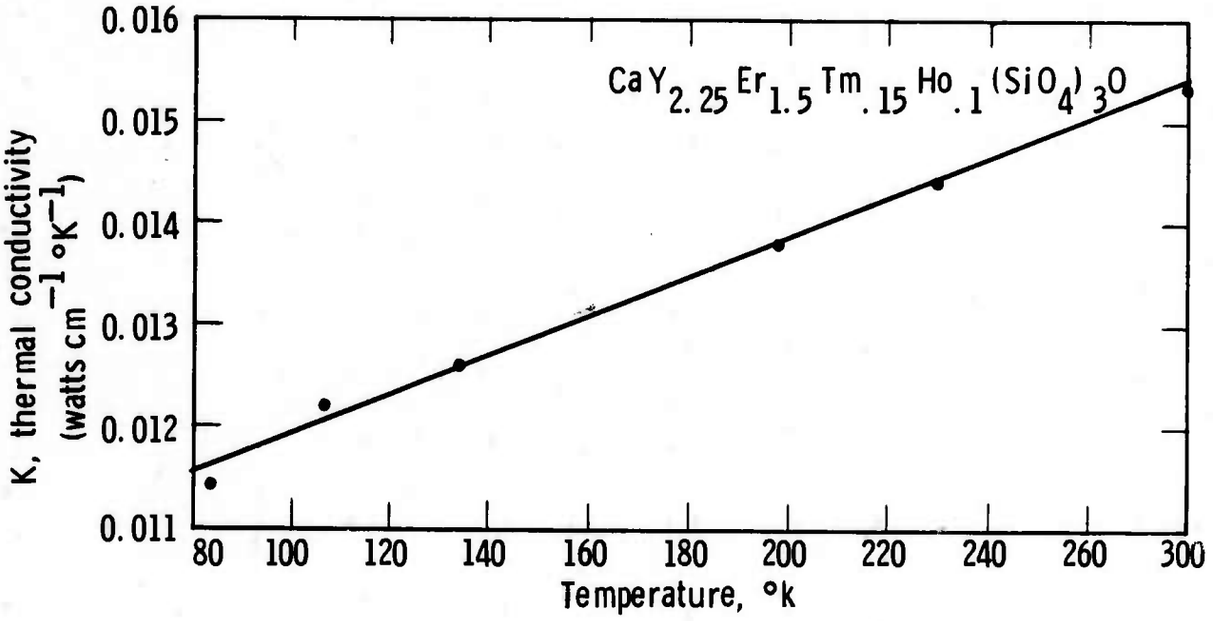

Fig. 3

Curve 594859-B

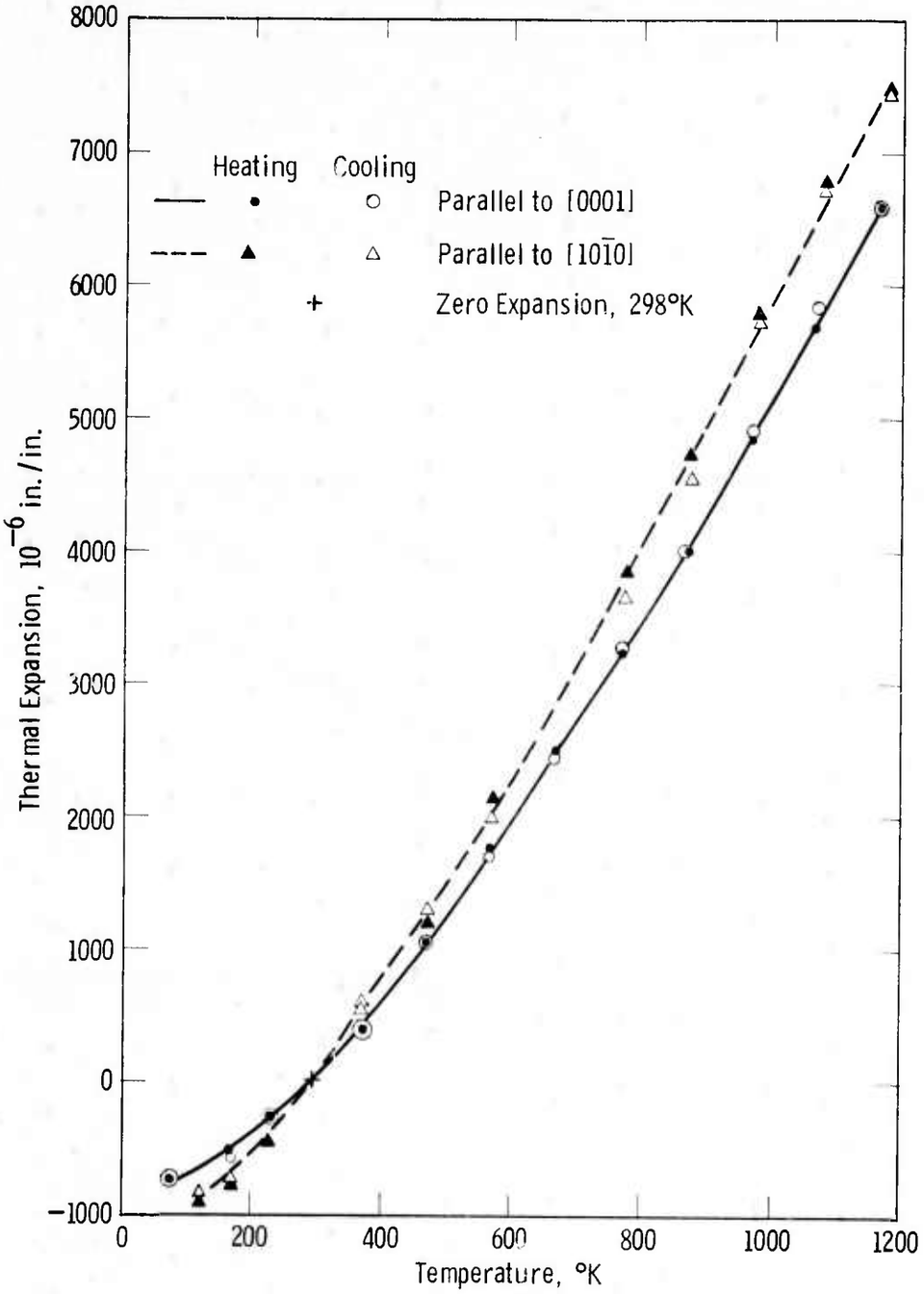

Fig. 4

3.1.2.1D Heat Capacity

The heat capacity of an 8.249g polycrystalline sample of $CaY_{2.25}Er_{1.5}Tm_{.15}Ho_{.1}(S.O_4)_3O$ was measured by means of the thermometer and calorimeter previously employed to measure the heat capacity of FAP crystals (Appendix II). A gram formula weight of 1650.1 was taken for the triply doped CaYSOAP corresponding to two formula weights per unit cell. Measurements were made at temperatures between 2.5 and 110°K, but recalibration of the thermometer indicated that the low temperature data was in error. The higher temperature data, presented below, is believed reliable within ± 10%.

T(°K)	Cp (cal $mole^{-1}$ $°K^{-1}$)
80.81	76.75
84.92	83.31
90.0	90.08
95.0	93.51
100.0	96.98
105.0	103.85
110.0	109.61

3.1.2.1E Space Group, Lattice Parameter and Density

Ito[12] performed X-ray diffraction analysis on powder samples of composition $CaY_4(SiO_4)_3O$. He was able to index the X-ray patterns on the basis of the established apatite hexagonal cell of space group $P6_3/m$. He calculated unit-cell dimensions from 10 reflections, each appropriately weighted. From his data he deduced lattice parameters a = 9.34A° and

c = 6.77 so that the unit cell volume is 511 $A^{\circ 3}$. We can obtain the theoretical or X-ray density of undoped CaYSOAP from the formula $\rho(\frac{g}{cm^3}) = \frac{1.66020\ \Sigma A}{V}$ [13] where A= sum of the atomic weights of the atoms in a unit cell and V= cell volume in A°.[3] The result of this calculation is ρ = 4.47 g/cc.

We are now in the process of confirming Ito's results and measuring the lattice parameters of doped CaYSOAP.

3.1.2.1F Hardness

We measured the hardness of a polycrystalline sample of triply-doped CaYSOAP which had been mounted in lucite and polished to present a flat surface to the hardness indenter. All measurements were performed on a Tukon Hardness Tester by means of a diamond indenter which was driven by a 200 g load. Hardness impressions were measured with a Filar microscope eyepiece and only those impressions which were free from specimen cracks were counted. The data were recorded in terms of Knoop Hardness Number (KHN) and the values tabulated below are the average of twenty measurements. An approximate correlation can be obtained between KHN and Moh hardness by use of the data of Knoop, Peters and Emerson[8] and these values are also listed. The data for YAG and FAP single crystals, included for comparison, were obtained in the same fashion as that for CaYSOAP.

Material	KHN(200g load)	Moh hardness
CaYSOAP, $CaY_{2.25}Er_{1.5}Tm_{.15}Ho_{.1}(S.O_4)_3O$	702±15	6.6
YAG, $Y_3Al_5O_{.2}$	1350±50	8.0
FAP, $Ca_5(PO_4)_3F$	500±20	5.6

The hardness of CaYSOAP is intermediate between those of FAP and YAG and hence, if hardness is assumed an indication of strength, we may expect CaYSOAP laser rods to withstand somewhat greater power densities, than can FAP, without failure. Indeed we have noted, qualitatively, that CaYSOAP crystals tend to crack much less readily than FAP when subjected to thermal shock, e.g., rapid cooling after growth

3.1.2.2 FAP:Ho, Cr

Physical property data for undoped and Nd-doped fluorapatite crystals have been compiled elsewhere.[7] Appendix I discusses in some detail the thermal properties of FAP important for laser system design considerations. We do not feel that replacement of Nd^{+3} by the Ho^{+3} ion in FAP should significantly change design considerations based on these properties, and hence the previously determined properties of FAP:Nd are listed for reference in Table 1 with those of CaYSOAP and YAG.

TABLE 1

The Physical Properties of FAP, CaYSOAP, and YAG

PROPERTY	FAP	CaYSOAP	YAG
Chemical Formula	$Ca_5(PO_4)_3F$	$CaY_4(SiO_4)_3O$	$Y_3Al_5O_{12}$
Crystal Structure	Hexagonal ($P6_3/m$)	Hexagonal ($P6_3/m$)	Cubic ($Ia3d$)
Lattice Constant(s), A°	a=9.3697±.0004 c=6.8834±0.0008	a=9.34 c=6.77	a=12.01
Melting point, °C	1645	2060	1970
Hardness Moh Knoop (200g load)	 5.6 500	 6.6 702	 8 1350
Density, g/cc	3.20	4.47	4.56
Hygroscopy	Nil	Nil	Nil
Solubility Water Common Acids	 Nil Moderate	 Nil Slight	 Nil Slight
Thermal Expansion Coeff, $°C^{-1}$ at R.T.	$[000\bar{1}]10\times10^{-6}$ $[10\bar{1}0]9.4\times10^{-6}$	$[000\bar{1}]5.7\times10^{-6}$ $[10\bar{1}0]7.1\times10^{-6}$	$[100]8.2\times10^{-6}$
Thermal Conductivity watts $cm^{-1}°C^{-1}$ at R.T.	$[000\bar{1}]0.022$ $[10\bar{1}0]0.019$	[0001] 0.016	0.12
Heat capacity, $\frac{cal}{gm°C}$	0.178, 296°K	0.0665, 110°K	0.140, 290°K
Refractive Indices at 6328A° η_o η_e	 1.634 1.631	 1.831 1.816	 1.82

3.2 SPECTROSCOPIC MEASUREMENTS

3.2.1 General Considerations

Most of the optical measurements required to optimize the composition of CaYSOAP have already been completed and described in the technical report issued at the end of the first six months of the program.[2] The majority of the optical measurements performed during this period, therefore, fell into two categories: those intended to delineate the optical characteristics of material under study and those designed to provide more detailed information on the material than could be obtained by conventional techniques. Those of the first kind included excitation and fluorescence measurements on all samples previously synthesized and optical transmission measurements of all boules to be fabricated into laser rods. These tests served to establish any gross differences between samples and also provided a non-destructive method for determining the concentration of doping ions. Most measurements on CaYSOAP fell into this first group.

The second type of measurements were confined mainly to FAP:Ho,Cr samples and were designed to investigate the nature of the Cr ion and Cr-Ho interactions in FAP. These studies included optical transmission measurements of FAP:Ho,Cr single crystals at 77°K and some preliminary electron spin resonance studies of Cr which are still in progress.

Some decay and transfer time measurements were also performed on various single and polycrystalline samples. Attempts to modify and improve the test apparatus led to some uncertainties in the data, and so they will not be reported at this time.

3.2.2 CaYSOAP:Er,Tm,Ho

3.2.2.1 Fluorescence Measurements

Fluorescence studies were carried out primarily on single crystal samples, and served to survey the material intended for laser testing. Measurements were made at 77°K and covered the spectral range 1.4 to 2.2 microns. One of the objectives of this work was to look for evidence of Er^{+3} or Tm^{+3} fluorescence which would indicate that energy transfer from these ions to Ho^{+3} was incomplete. The fluorescence if present would occur at 1.55μ (Er^{+3}) and 1.8μ (Tm^{+3}).

Figures 5 and 6 depict typical results from crystals to be fabricated into laser rods. The sensitivity of the instrument is about twenty times greater in the range 1.4 to 1.9μ than in the range 1.9 to 2.2μ in order to magnify the effects of Er^{+3} or Tm^{+3} fluorescence. No evidence for such fluorescence is present in these spectra or spectra obtained from any of our laser crystals. This indicates that the Ho^{3+} content of the crystals is sufficiently great to ensure complete energy transfer to Ho^{+3} from both Er^{+3} and Tm^{+3}.

Although the nominal compositions of the crystals whose spectra appear in figures 5 and 6 was the same, there is a difference in the ratio of the dominant peaks at 2.06 and 1.95μ between the two figures. Sample #18-20330 (Fig. 6) represents a lower limit for this ratio at the indicated Ho^{+3} content, while sample #108-203380 (Fig. 5) is more typical of other crystals studied. There are several possible causes for this phenomenon. For example, we have noted in general that increasing the Ho^{+3} concentration increases the intensity of the longer wavelength peak relative to the 1.95μ peak. This is true for CaYSOAP and FAP as well.

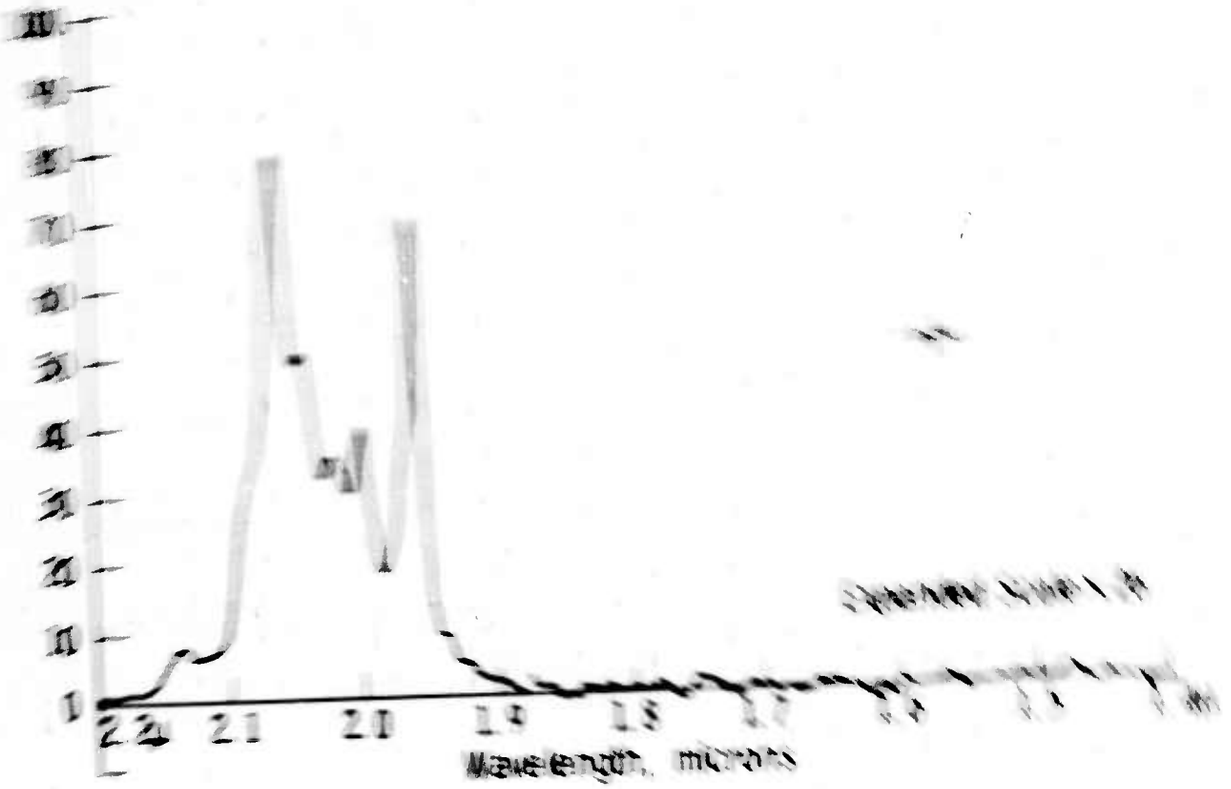

Fig. 3

Curve 594892-A

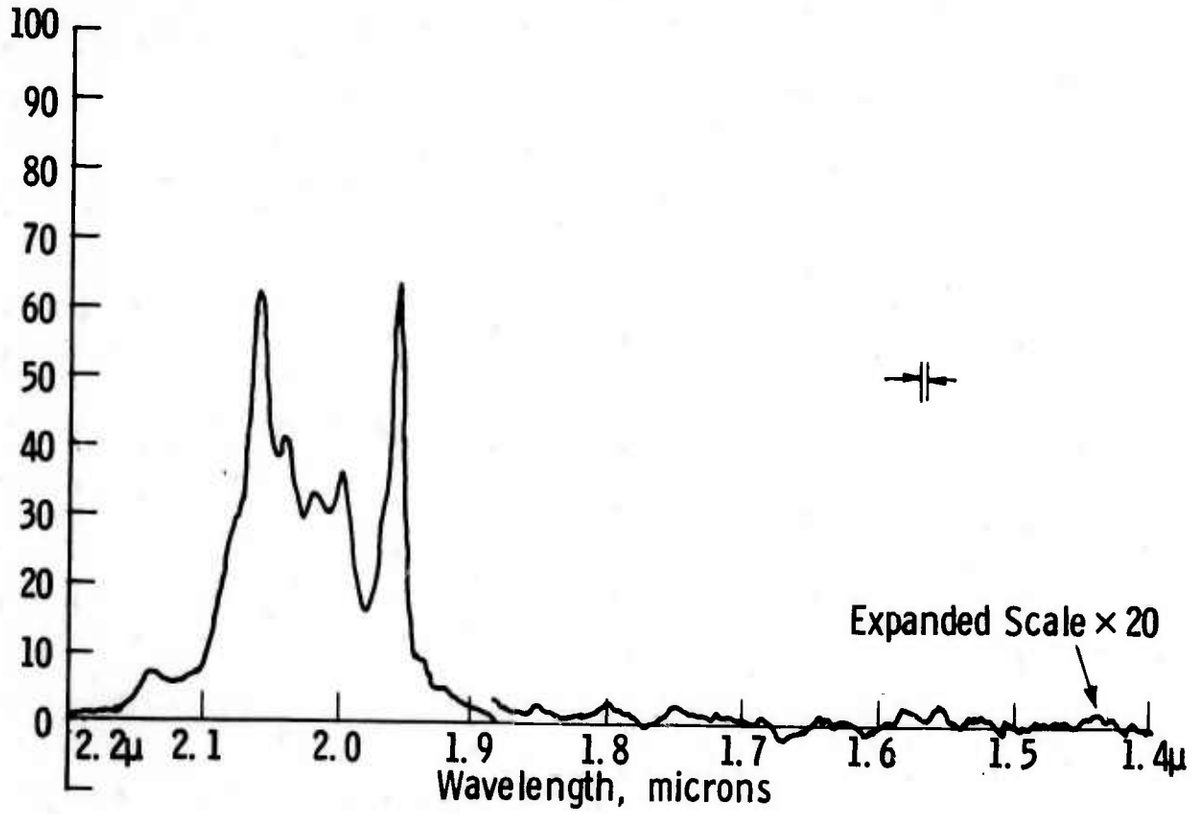

Fig. 6

It could indiate ion-ion interactions occurring at the higher concentrations. A second reason could be connected to differences in site occupancy. We feel that variations in Ho^{+3} content and differences in site occupancy for Ho^{+3} are both possible to some degree and could account for the observations discussed above, but at the moment we have no data to indicate the extent to which either occurs.

Although orientation effects cannot explain the differences between Figures 5 and 6, crystal orientation does affect the intensity of fluorescence. For example, when Nd^{+3} is the dopant, the fluorescence intensity of the 1.06μ line from FAP crystals differs by a factor of 2.5 between the a and c orientations.(7) Such differences in intensity with orientation are significant with regard to laser performance inasmuch as they partially determine the laser gain near threshold. This in turn influences the choice of direction for crystal growth.

Figures 7 and 8 compare the fluorescence in the c and a-axis directions for a triply-doped CaYSOAP crystal pulled in the c direction. The crystal was cut and polished to provide pairs of a and c faces of approximately equal area with the crystal thickness normal to each pair of faces sufficient to completely absorb all of the excitation radiation from about 0.3 to 1.2μ. The radiation incident on the sample was essentially unpolarized. Amplifier gain and other conditions were identical for both measurements.

Examination of Figures 7 and 8 shows that the c-direction fluorescence is more intense than that of the a-direction, but only by

Curve 594893-A

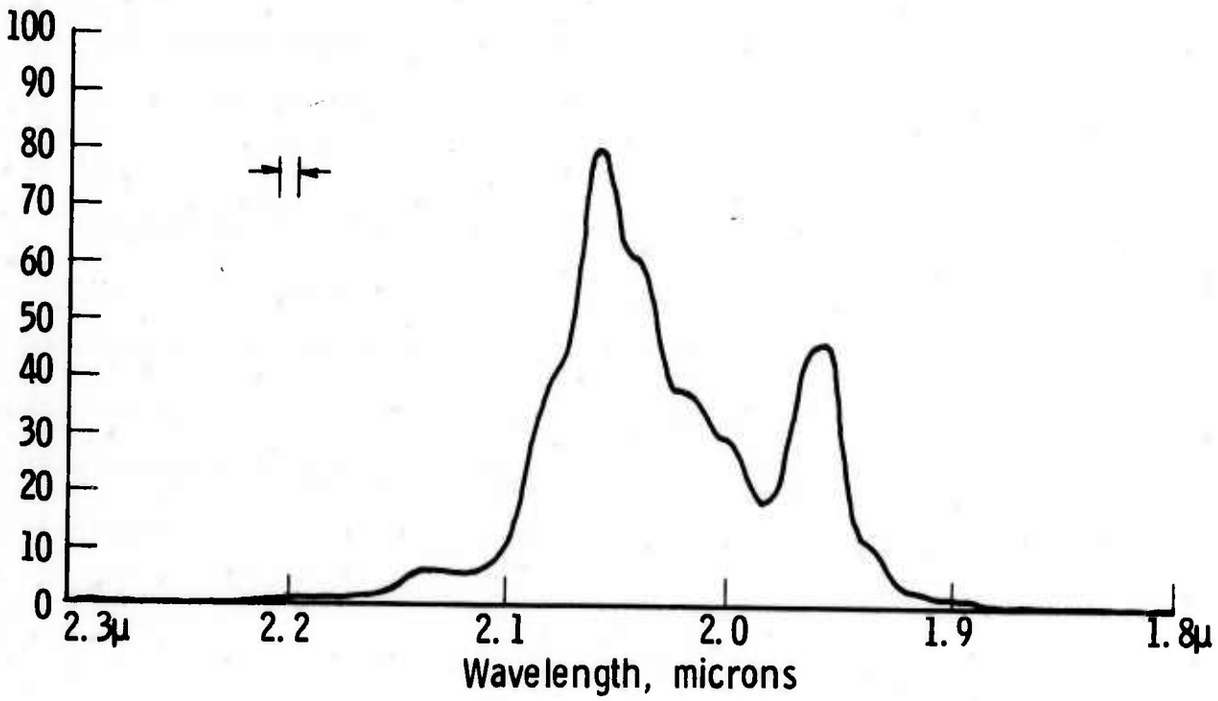

Fig. 7

Curve 594894-A

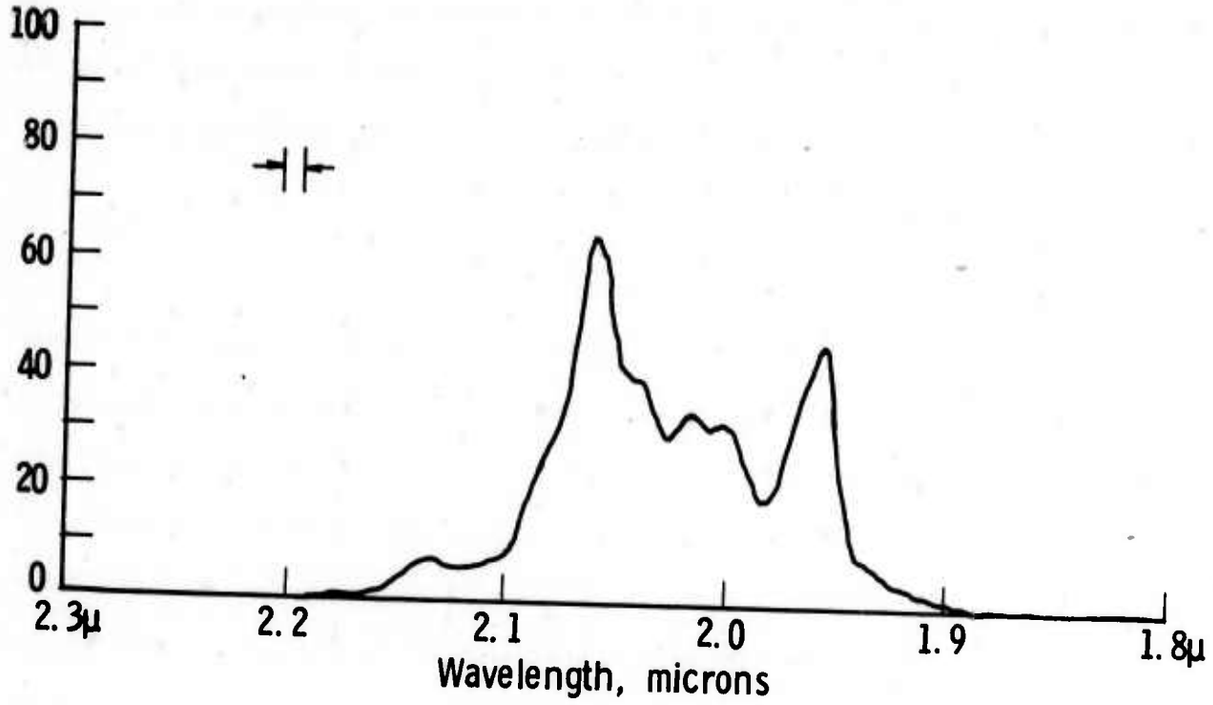

Fig. 8

about thirty percent, much less than that in FAP:Nd.[7] (The c direction corresponds to the direction of growth for all CaYSOAP crystals studied so far.) A closer scrutiny of figures 7 and 8 reveals that the difference in fluorescence intensity for the two directions occurs entirely in the 2.06μ line, but that differences in shape can be seen in the 1.95μ line, as well as in the shoulders of both main lines. These differences are perhaps related to the occupancy, by Ho^{+3}, of sites having different symmetries.

3.2.2.2 Excitation Measurements

We have obtained the excitation spectra of most of the polycrystalline and single crystal samples of CaYSOAP:Er,Tm,Ho synthesized during the course of the program. These spectra reveal few unexpected features; their general characteristics were discussed previously.[2]

Figures 9 and 10 show the excitation spectra for CaYSOAP:Er,Tm,Ho and YAG:Er,Tm,Ho. The Ho concentration of CaYSOAP is somewhat lower than our typical laser samples while the YAG sample is a commercial laser rod whose rare-earth contents are not known. Judging from published data,[9] however, the YAG sample contains a considerably higher concentration of rare-earth ions than does the CaYSOAP sample. Despite the expected concentration differences between the samples, the two spectra are quite similar. Gaps appear in each spectra which are centered at approximately 0.58, 0.73 and 0.9μ. A gap also occurs at 1.35μ (not shown on these figures).

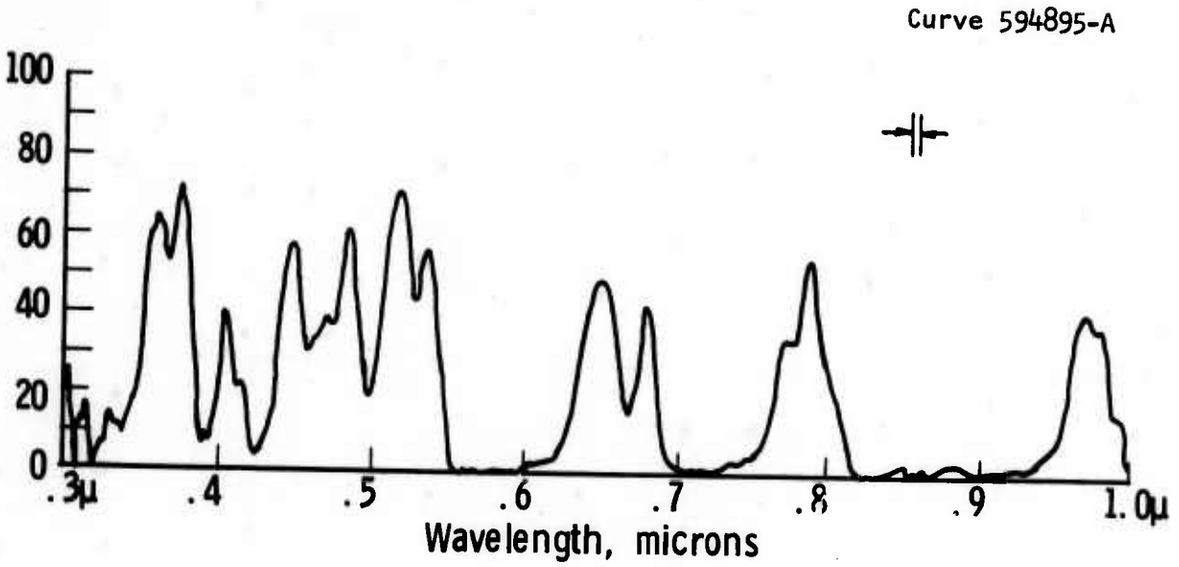
Curve 594895-A
100
80
60
40
20
0
.3μ
.4
.5
.6
.7
.8
.9
1.0μ
Wavelength, microns

Fig. 9

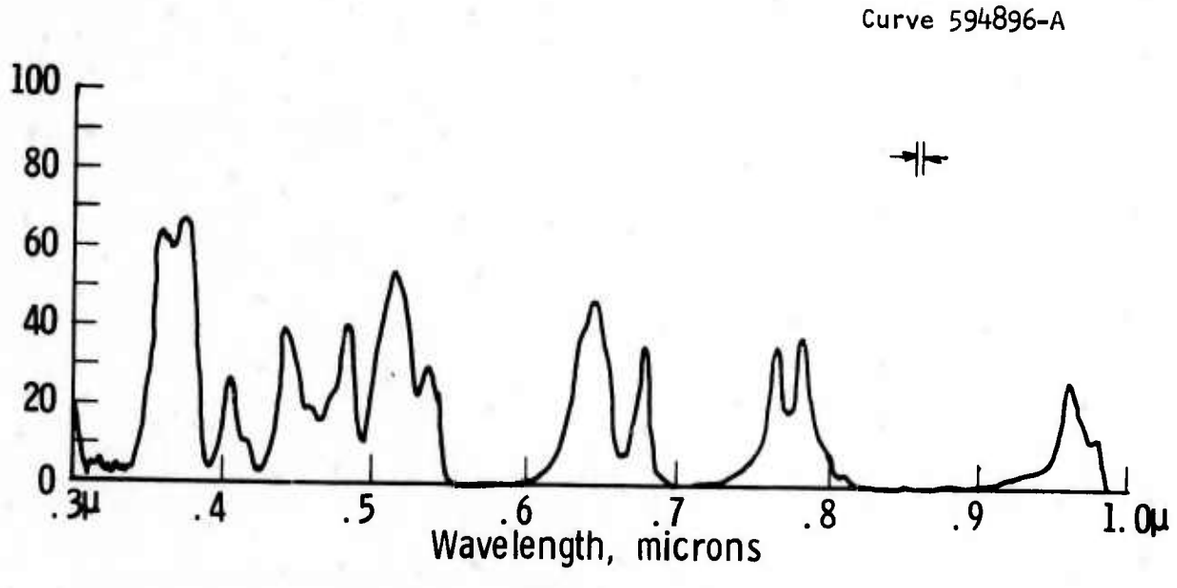
Curve 594896-A
100
80
60
40
20
0
.3μ
.4
.5
.6
.7
.8
.9
1.0μ
Wavelength, microns

Fig. 10

3.2.2.3 Transmission Measurements

All optical density measurements were performed on crystals to be fabricated into laser rods. The measurements were performed prior to fabrication in order to verify that the rare-earth ion content of each sample was correct. Transmission measurements also reveal excessive optical scattering and the presence of unwanted impurity ions. As in the case of the excitation spectra, our most recent transmission data are very similar to those previously reported.[2] We are, however, also using quantitative transmission measurements in conjunction with chemical analysis of pulled crystals in order to obtain the absorption cross sections of Er^{+3}, Tm^{+3} and Ho^{+3} in CaYSOAP. With this data we can quantitatively, and in a non-destructive manner, measure the rare earth contents of each laser crystal grown.

3.2.3 FAP:Ho,Cr and FAP:Cr*

3.2.3.1 Fluorescence Measurements

We measured the fluorescence spectra of FAP:Ho,Cr samples synthesized during this program as well as those of some older spectroscopic samples[1] in order to confirm the observation that the longer wavelength four-level transition is favored over the transition to the ground state at higher Ho^{+3} concentrations (section 3.2.2.1). Figure 11 shows that this observation does indeed hold for FAP as well as CaYSOAP.

---

*Some of the earlier information on the properties of this material was embodied in a paper entitled "FAP:Ho,Cr - A New Infrared Laser Material" presented by N.T. Melamed at the 1970 International Quantum Electronics Conference, Kyoto, Japan.

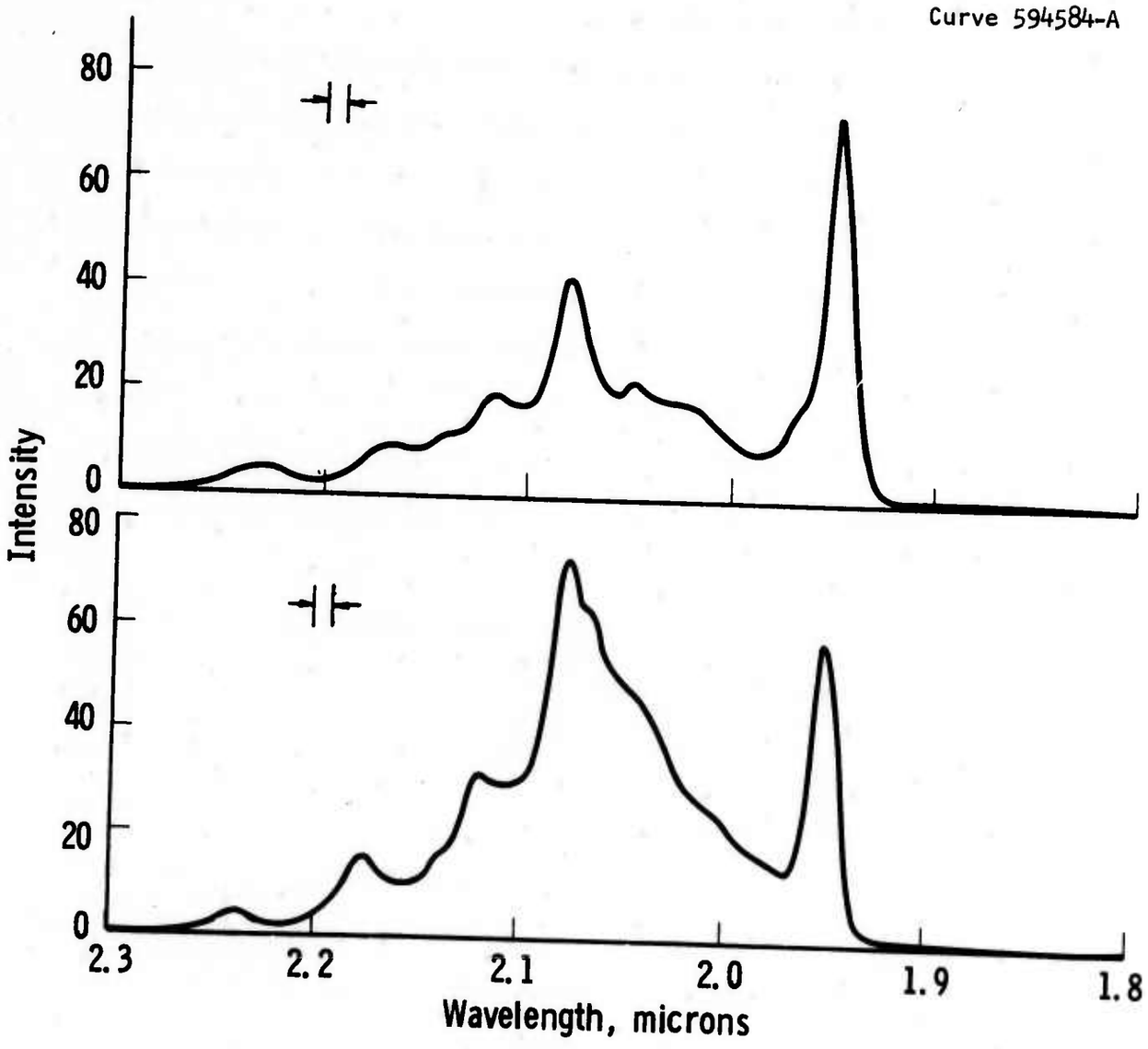
Curve 594584-A
80
60
40
20
0
Intensity
80
60
40
20
0
2.3
2.2
2.1
2.0
1.9
1.8
Wavelength, microns

Fig. 11

Most other fluorescence measurements on FAP:Ho,Cr were made in conjunction with an investigation of the nature of the Cr ion in FAP. We looked for evidence of Cr fluorescence in samples containing only Cr, but were unable to detect any such fluorescence over the wavelength range from 0.4 to 2.1μ either at 77°K or room temperature.

3.2.3.2 Excitation Measurements

Excitation data on FAP:Ho,Cr is presented in the previous report.[2]

3.2.3.3 Transmission Measurements

As in the case of CaYSOAP:Er,Tm,Ho, we measured the spectral transmission of FAP:Ho,Cr crystals prior to their fabrication into laser rods. In addition, a number of studies were performed on crystals of FAP containing specially chosen concentrations of Ho and Cr or Cr alone. These consisted of a and c axis transmission measurements using plane polarized light with sample temperatures held at 77°K and room temperature.

All of the measurements were taken with a Cary 14CMR recording spectrophotometer whose light was polarized by means of matched Glan-Thompson prisms inserted into the sample and reference beams. The prisms used in our work limited short wavelength measurements to 3600 Å. Samples were cooled to 77°K in a He dewar, model CD-151, designed by Union Carbide Corporation for use with the Cary instrument.

Figure 12 depicts the optical absorption of a lightly doped FAP:Cr sample at 77°K. Both polarizations are shown for light propagating

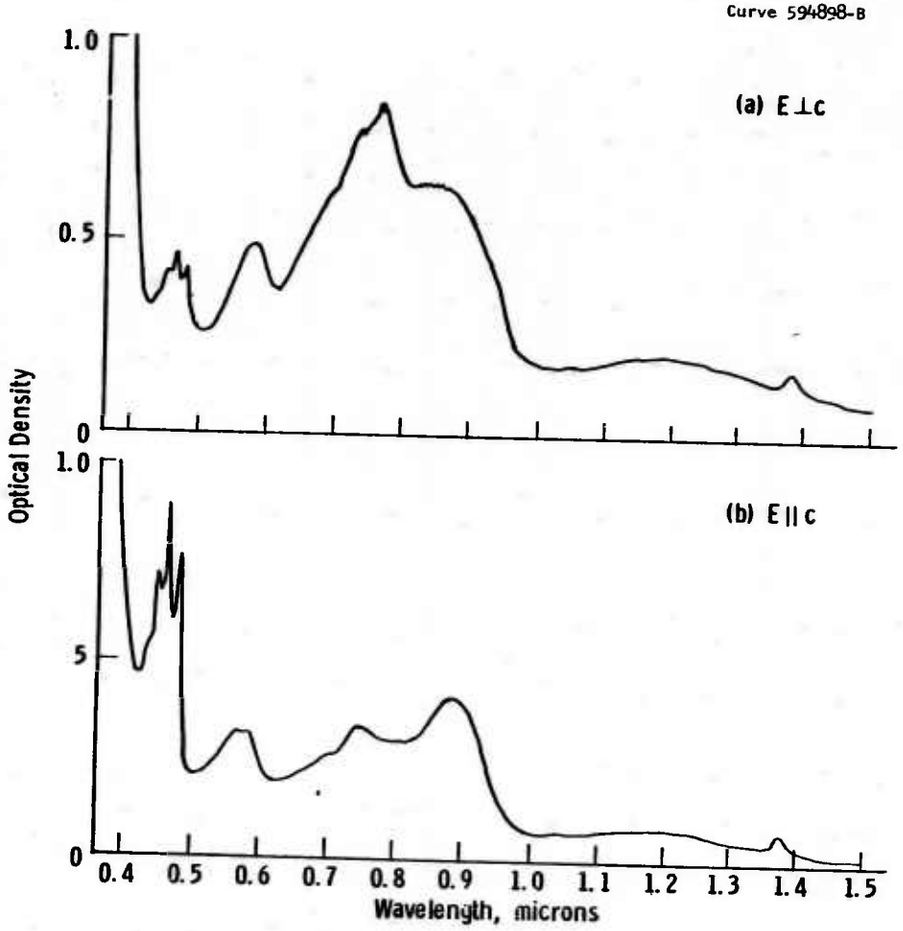
Curve 594898-B
1.0
0.5
0
(a) E⊥c
1.0
5
0
(b) E∥c
Optical Density
0.4
0.5
0.6
0.7
0.8
0.9
1.0
1.1
1.2
1.3
1.4
1.5
Wavelength, microns

Fig. 12

along the a axis. The E $\perp$ c spectrum is similar to that obtained with light propagating parallel to c, indicating the electric dipole character of the optical transitions. The absorption spectra of FAP doped with Ho and Cr is shown in Figure 13. The sharp absorption lines of Ho^{+3} are easily distinguished from the rather broad bands due to the Cr ion.

Although we have not as yet attempted to carefully analyze the optical spectrum of Cr in FAP, some interesting features were noted. First, there are a large number of bands due to Cr (at least seven can easily be distinguished) in the spectral region studied. Second, cooling samples to 77°K has very little effect on the positions, widths, or intensities of these bands. The most pronounced change produced in the transmission spectrum at 77°K is a slight narrowing of the band at 0.76μ and the development of three poorly resolved bands (near 0.58μ) which appear as a single band in the room temperature spectrum. Of greatest significance with respect to energy transfer from Cr to Ho^{+3} is the fact that most of the absorption lines of Ho^{+3} fall within the range of a Cr absorption band, often, in fact, near the peaks of the Cr bands. This broad overlap in the transition energies of the two ions probably accounts for most of the good transfer yields from Cr to Ho.

We hope in the near future to be able to analyze the properties of the Cr ion in FAP in a more detailed fashion.

3.2.3.4 Measurement of Cr Paramagnetic Resonance*

Spin resonance measurements were performed on a moderately doped single crystal of FAP:Cr. The objective was to provide additional insight into the nature and properties of the Cr ion in FAP. Measurements

*These measurements were performed by Dr. George Wagner of our Laboratories.

Curve 594897-A

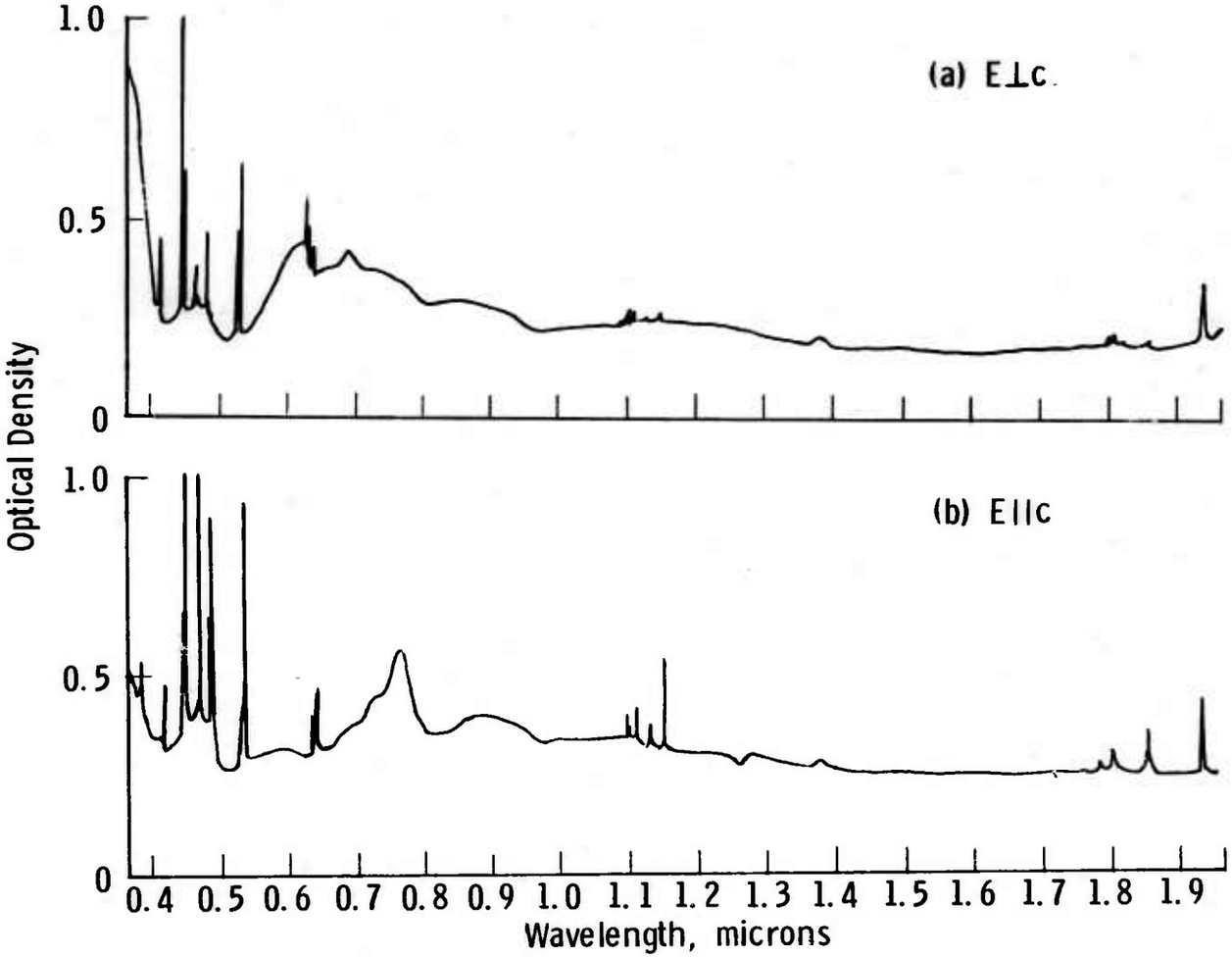

Fig. 13

were performed at 77°K only, and a map of the results obtained is shown in Figure 14. Six resonances are observed in a general direction. These are degenerate to within the resolution of the experimental arrangement for the magnetic field along the a and c axes. The number of lines observed and the g values are consistent with an interpretation of the data assuming Cr ions at the sites of distorted tetrahedra. The most reasonable explanation for this is that Cr^{+5} is substituting for P^{+5} in the $(PO_4)^{-3}$ tetrahedra of the fluorapatite lattice. A similar substitution is found in spodiosite, i.e., $Ca_2(PO_4)Cl$ in which Cr is present as $(CrO_4)^{-3}$ ions.[10] Since FAP crystals have rotational symmetry only about the c axis, no degeneracy, in general, should be observed during rotation of the magnetic field about the a axis. We therefore must assume that the observed degeneracy in FAP is accidental and arises because the g tensor is oriented such that its intersection with the a plane is a circle. The validity of this assumption is being investigated by further measurements.

Curve 594585-A

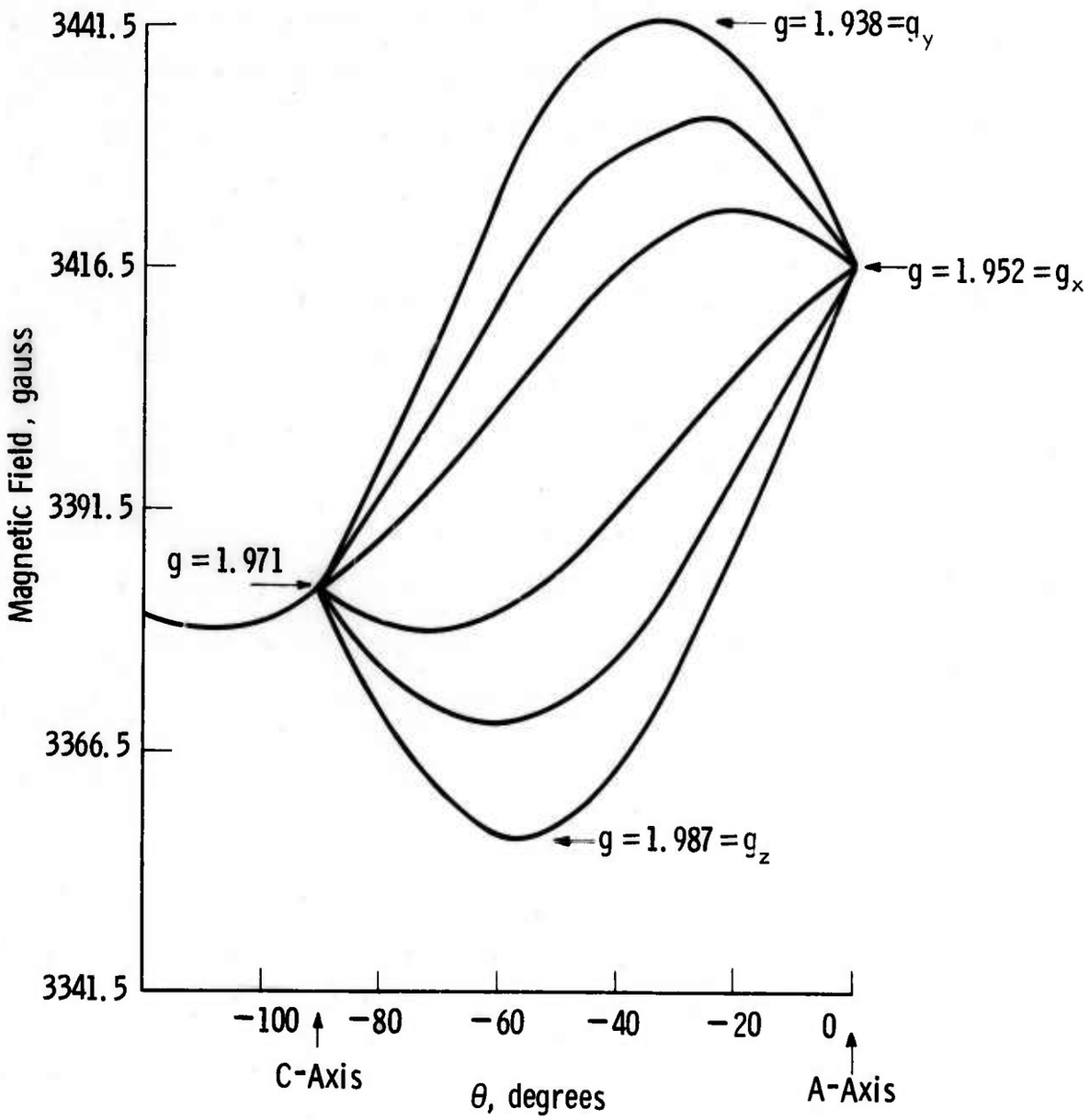

Fig. 14

3.3 LASER TESTS

3.3.1 General Considerations

Laser action has been obtained from both triply-doped CaYSOAP and FAP:Ho,Cr crystals. Most of the measurements described below pertain to CaYSOAP, since a greater proportion of our effort in the early stages of the program was devoted to preparation and growth of this material. Growth of FAP:Ho,Cr was resumed during this report period, but the laser results for these crystals are somewhat limited because some crystals failed to lase.

CaYSOAP was tested long pulse, Q-switched and CW and exhibited laser action in the first two modes of operation. Tests on FAP:Ho,Cr were confined to the long pulse mode only. To verify the consistency of our measurements and obtain a comparison of CaYSOAP and FAP with another state-of-the-art holmium laser, we also tested two rods of rare-earth sensitized, Ho- activated YAG, obtained commercially. The data pertaining to the YAG crystals are discussed in the sections devoted to CaYSOAP in order to facilitate the comparison of the materials.

The liquid nitrogen-cooled laser head previously described[2] was used for all measurements reported here. An Xe 1-1.5 flashlamp was used to pump the laser rods during long pulse and Q-switch tests. The pump pulse, approximately triangular in shape, had a rise time of about 0.5 msec and a total length of 1.5 msec. A Sylvania 800 W DXV Tungsten Iodine lamp was used for CW measurements. The flexibility provided by

the use of external resonators with this laser head made possible conventional threshold versus reflectivity measurements on CaYSOAP as well as the determination of the laser wavelength of this material by the frequency doubling experiments which are described in section 3.3.2.4 and Appendix II (this work has been submitted for publication).

3.3.2 CaYSOAP:Er,Tm,Ho

3.3.2.1 Long Pulse Measurements

Six CaYSOAP and two YAG rods were long pulse tested. We measured the threshold input to the flashlamp and the energy output of each rod as a function of output resonator reflectivity.

The double pass transmission and loss coefficient for each rod were determined from the threshold energies by the method described in References 2 and 11. As pointed out in Reference 11, we must know the relationship between the input energy to the lamp and its pump efficiency to obtain correct loss values. We have assumed that the excitation of the laser rod is proportional to the electrical energy stored on the discharge capacitor for all laser data presented below. This assumption may lead to loss coefficients that are somewhat high, although the method still yields data suitable to evaluate differences between crystals and to show trends in crystal quality.

We first tested an unsensitized CaYSOAP:Ho rod which had been grown prior to the start of this program. This rod fractured due to the steep temperature gradient along the rod as it was cooled to 77°K. The laser head was modified and the problem eliminated.

Each of the next three rods tested was sensitized with Er and

Tm. The output-input energy characteristics and threshold-reflectivity curves for these crystals are given in Figures 15 through 20. These data are also presented in summary form in Table 2.

We note from Table 2 that the double pass transmission of the CaYSOAP:Er,Tm,Ho rods is 50 to 60%. This corresponds to a loss of about 10 to 15% per cm. While the absolute values of the losses may be a bit high as mentioned above, they do reflect the presence of the second phase scattering defects in these early crystals (section 3.1.1.1), and to a lesser extent the lack of anti-reflection coatings on the rod ends. The latter may contribute to losses depending upon the rod alignment.

The slope efficiencies of the CaYSOAP crystals range from 0.04 to 0.17 with 95% output reflectivity and 0.21 to 0.61 with 55% output reflectivity. The slope efficiency of the 3 mm diameter rod, #18-203380, is lower than the efficiencies of the two 6.2 mm diameter rods, #108-203381 and 68-203380, by about the amount we would predict from the differences in rod cross-sectional area. This indicates that the 3 mm diameter rod is optically thin though slight differences in rod doping make direct comparisons between the rods difficult.

The threshold values for CaYSOAP at nitrogen temperature range between 28 and 79 joules depending upon the output coupling.

When we tested the two sensitized YAG:Ho rods under similar conditions to those used to test CaYSOAP (Figs. 21 to 24) we found that the YAG crystals had thresholds about one-tenth of those of CaYSOAP, losses of 1 to 4% per cm and slope efficiencies in the range

Table 2. Laser Test Results for Ho-Activated CaYSOAP and YAG

Rod No.	Dimensions mm Dia.	Length	Output Mirror Reflectivity %	Threshold Joule	Slope Efficiency %	Double Pass Transmission %	Loss Coefficient % cm^{-1}	Comments
SOAP #113-202867 $CaY_{2.9}Er_{0.9}Tm_{0.1}Ho_{0.1}$	5.4	38	-	-	-	-	-	Rod broken while being cooled.
SOAP #18-203380 $CaY_{2.9}Er_{0.9}Tm_{0.1}Ho_{0.1}$	3	25	95 75 55	28 34 41	0.04 0.11 0.21	47	15	
SOAP #108-203381 $CaY_{2.25}Er_{1.5}Tm_{0.15}Ho_{0.01}$	6.2	27	95 75 55	31 37 48	0.17 0.51 0.61	51	13	
SOAP #68-203380	6.2	25	95 75 55	56 69 79	0.12 0.36 0.44	61	10	
SOAP #77-203380 $CaEr_{3.9}Ho_{0.1}$	3.3	17	99.9					Did not lase with 120 joule input
SOAP #77-203380 $CaEr_{3.9}Ho_{0.1}$	3.55	20	99.9					Did not lase with 120 joule input.
ABC YAG #170y	3	30	95 75 55	3 5 6	0.75 1.25 1.20	(75)*	(4)	
ABC YAG #17284c	3	30	95 75 55	1.6 2.5 3.2	0.31 0.63 0.81	(93)	(1)	

*Data in parentheses are approximate.

Curve 594882-A

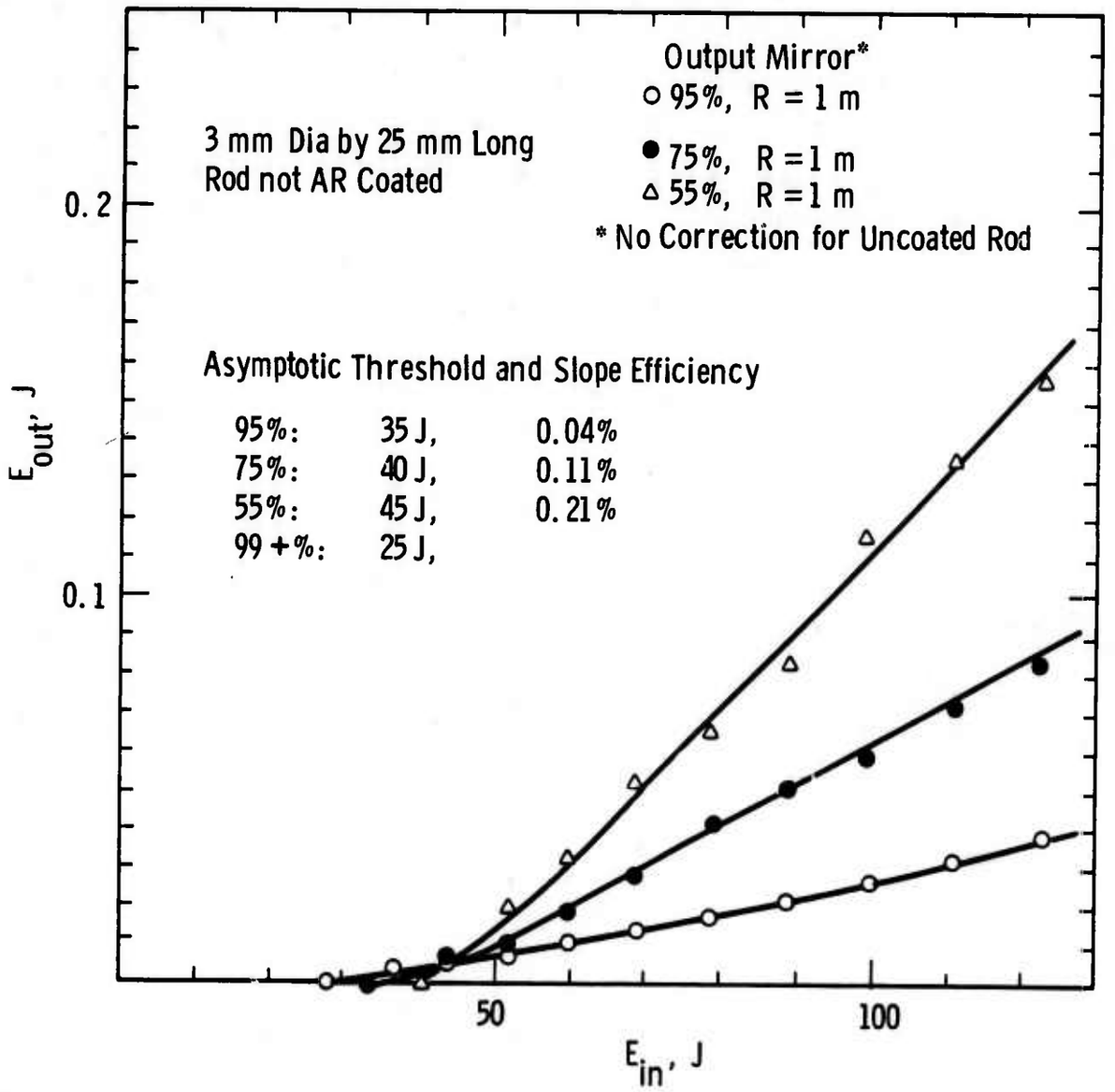

Fig. 15

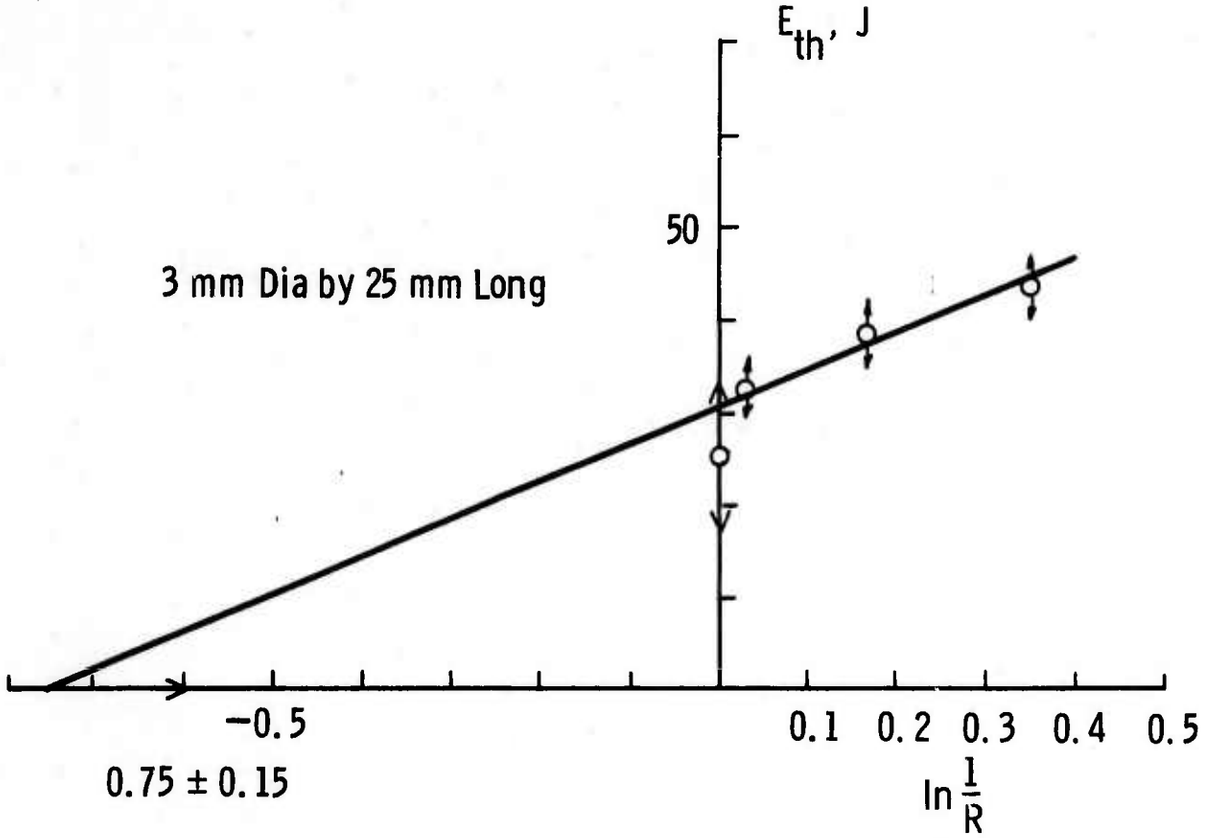
Curve 594876-A
E_{th}, J
50
3 mm Dia by 25 mm Long
−0.5
0.75 ± 0.15
0.1
0.2
0.3
0.4
0.5
$\ln \frac{1}{R}$

Fig. 16

Curve 594873-A

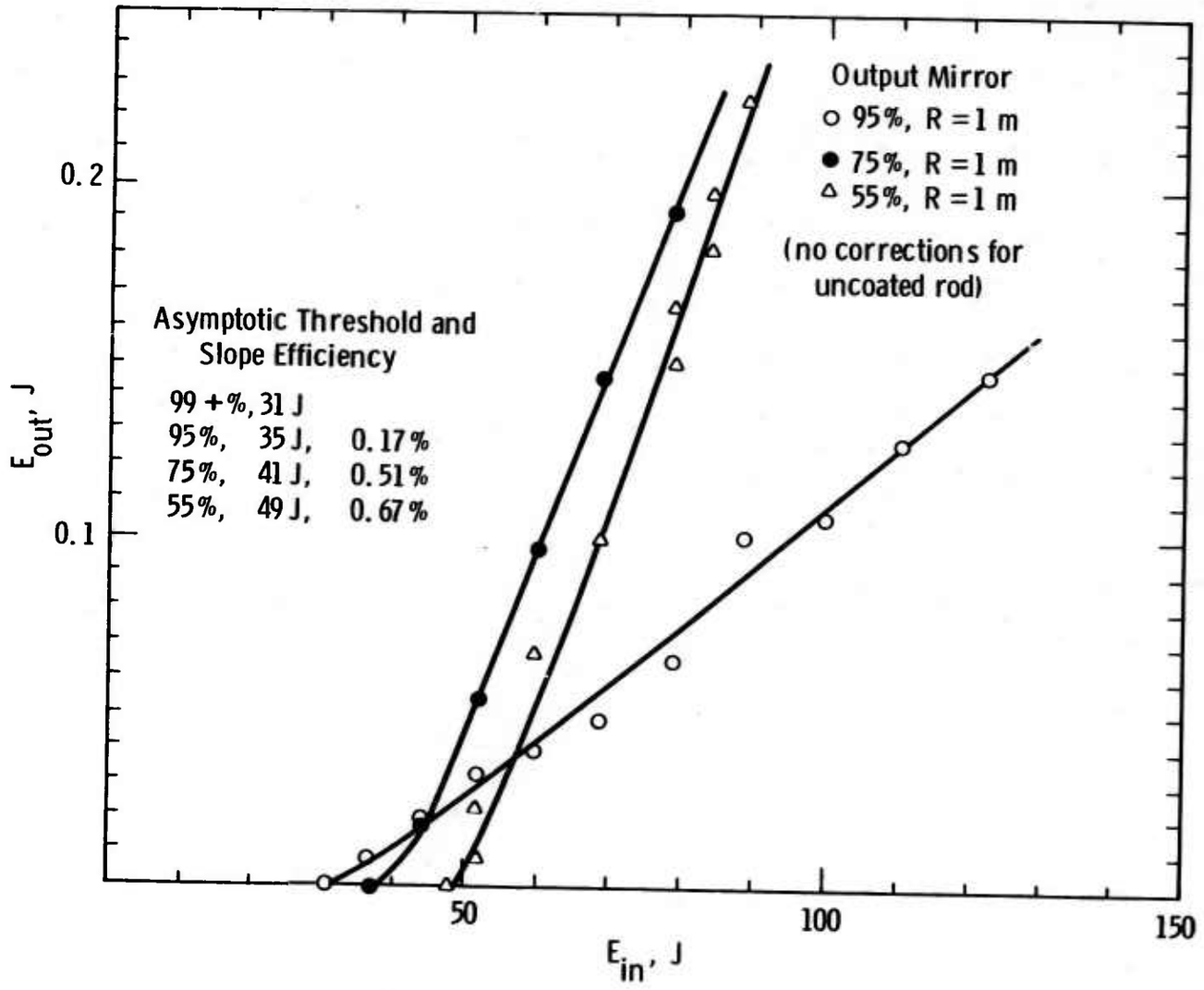

Fig. 17

Curve 594879-A

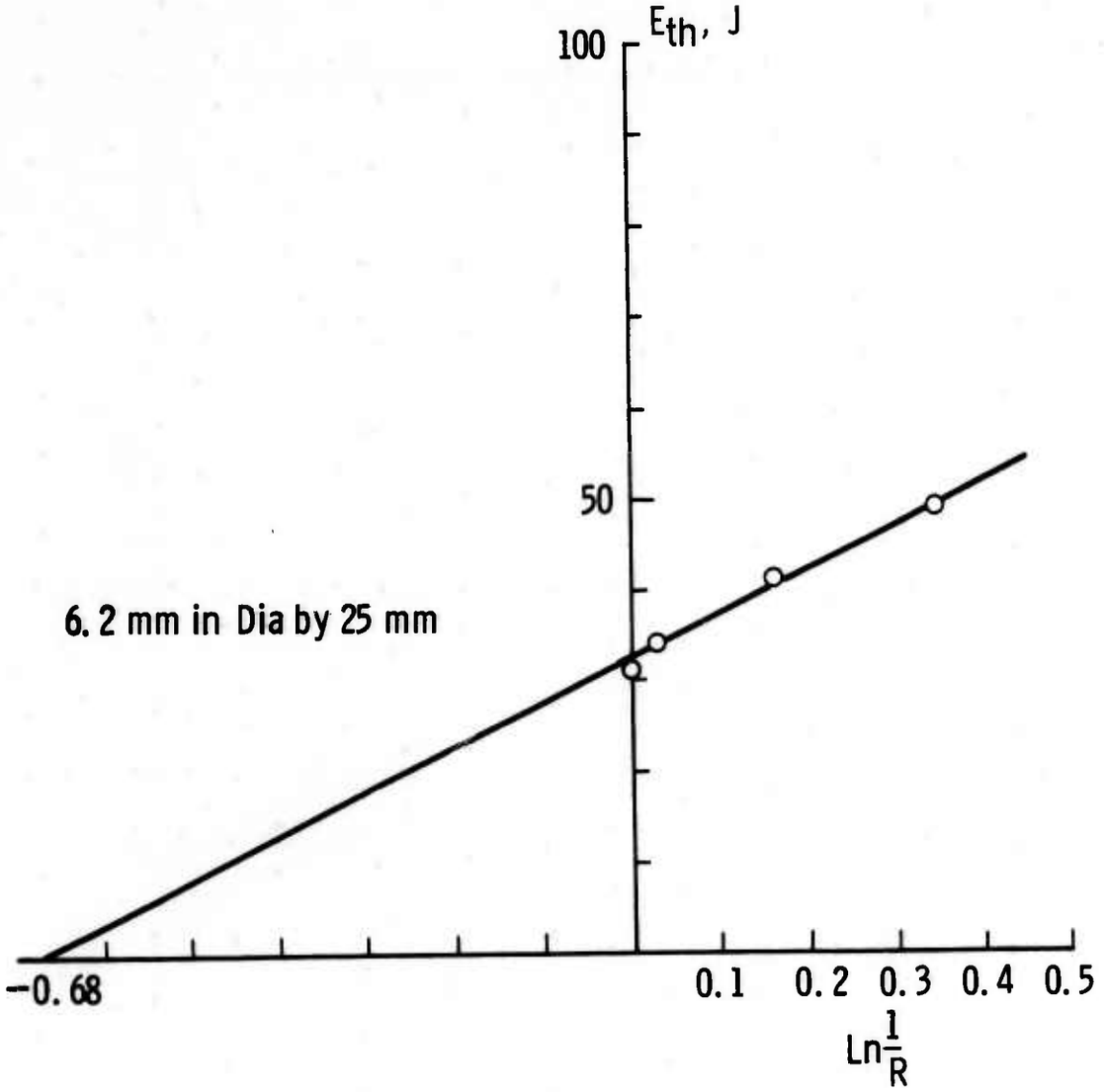

Fig. 18

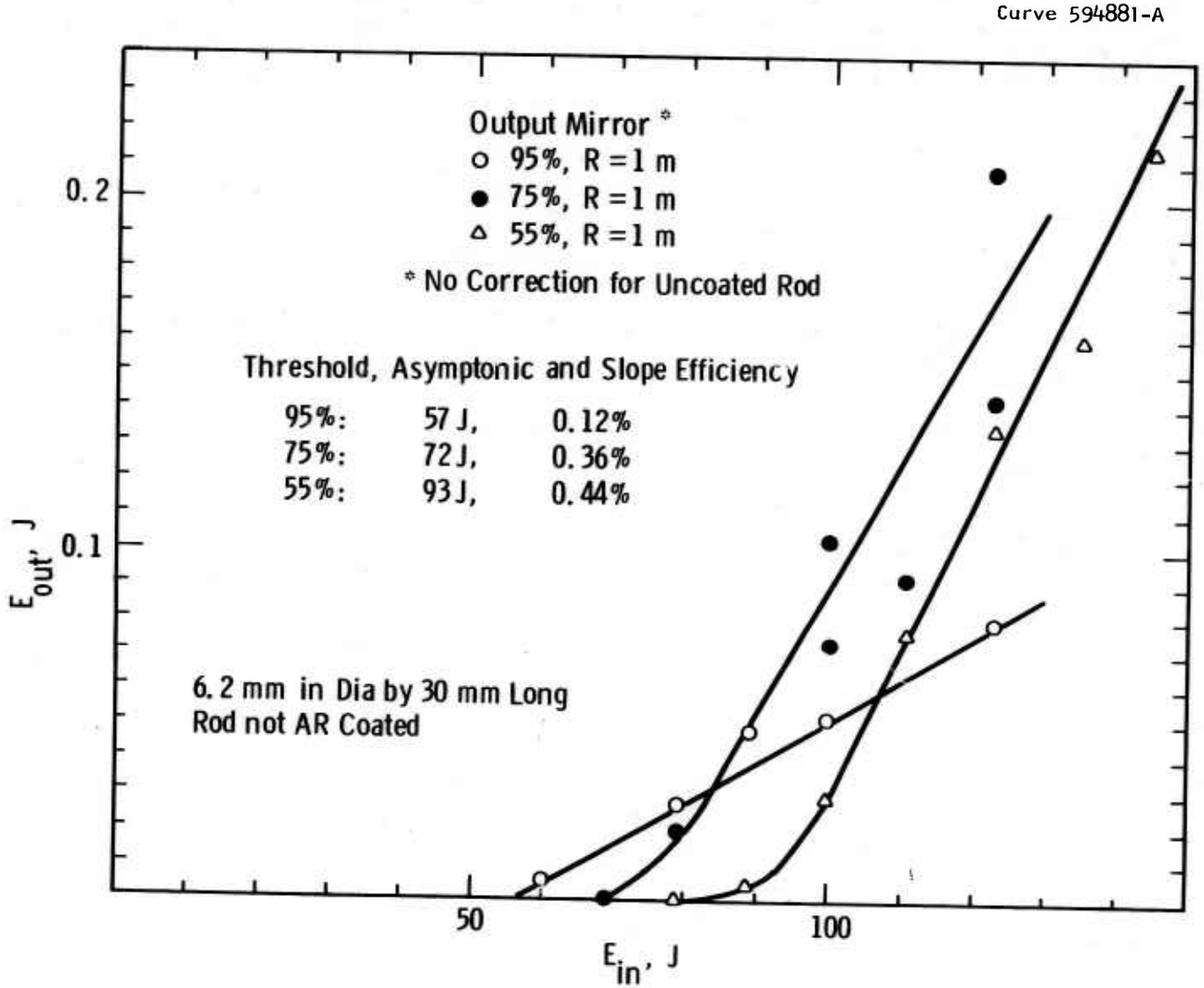
Curve 594881-A
Output Mirror *
○ 95%, R = 1 m
● 75%, R = 1 m
△ 55%, R = 1 m
* No Correction for Uncoated Rod
Threshold, Asymptonic and Slope Efficiency
95%: 57 J, 0.12%
75%: 72 J, 0.36%
55%: 93 J, 0.44%
6.2 mm in Dia by 30 mm Long
Rod not AR Coated
0.2
0.1
E_{out}, J
50
100
E_{in}, J

Fig. 19

Curve 594878-A

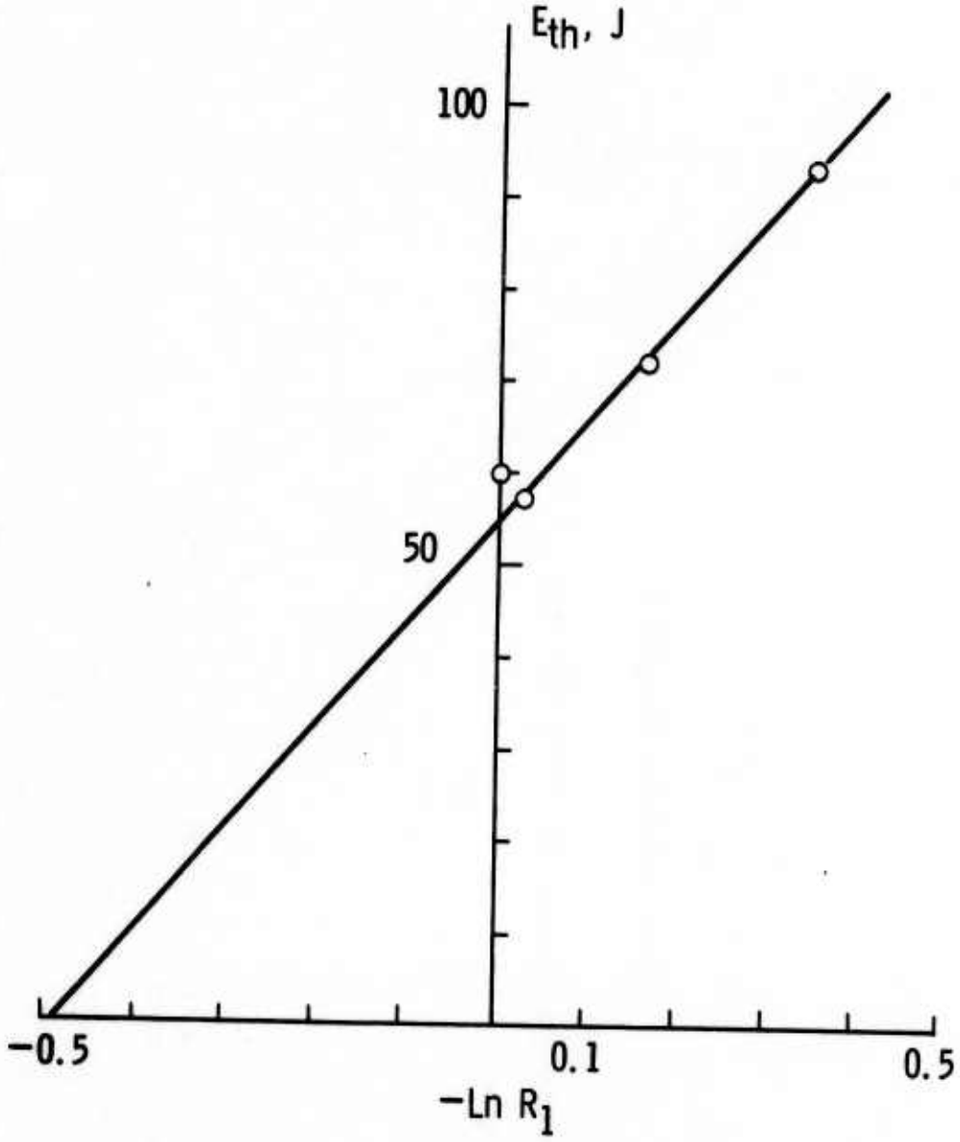

Fig. 20

Curve 594883-A

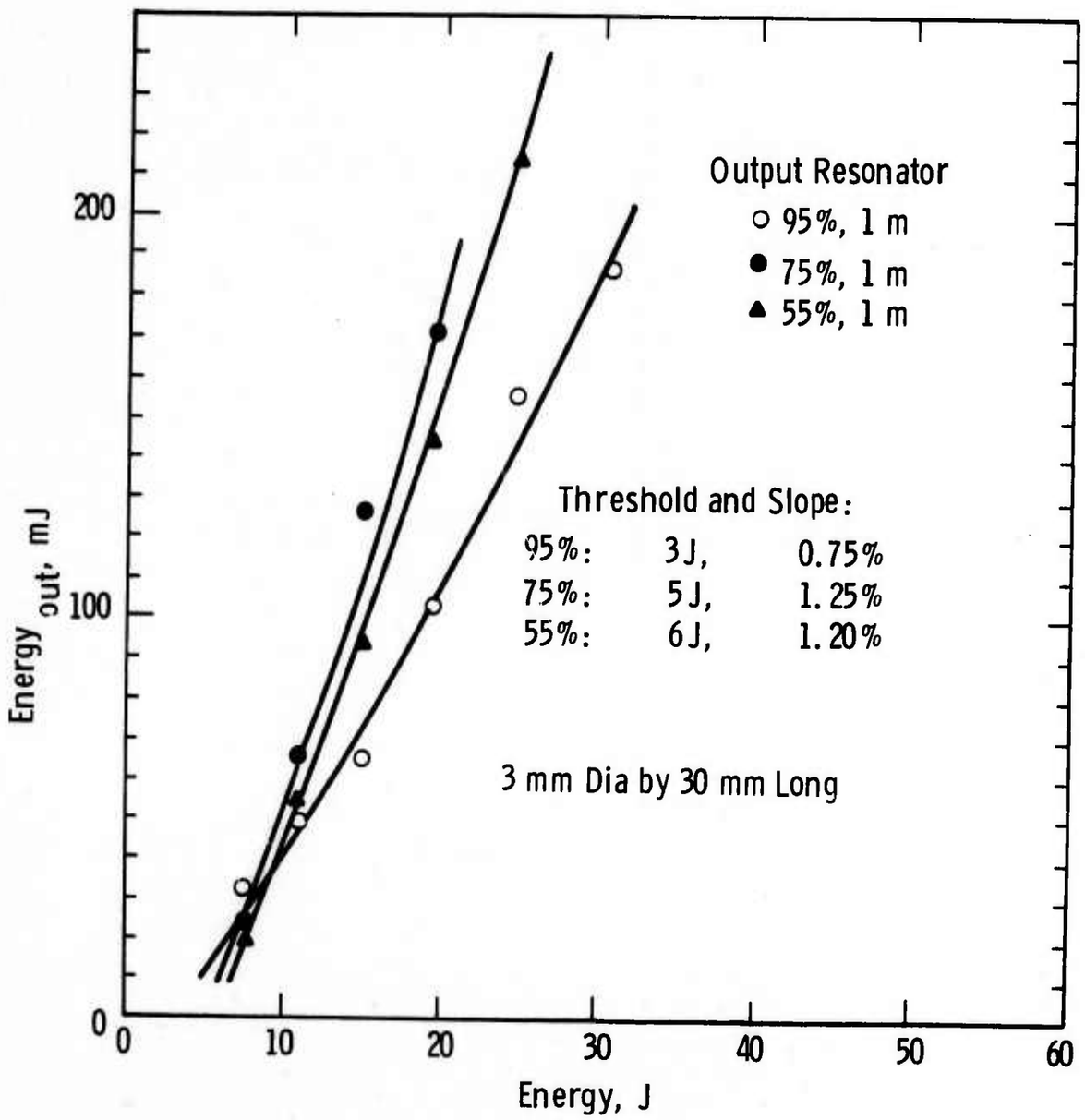

Fig. 21

Curve 594875-A

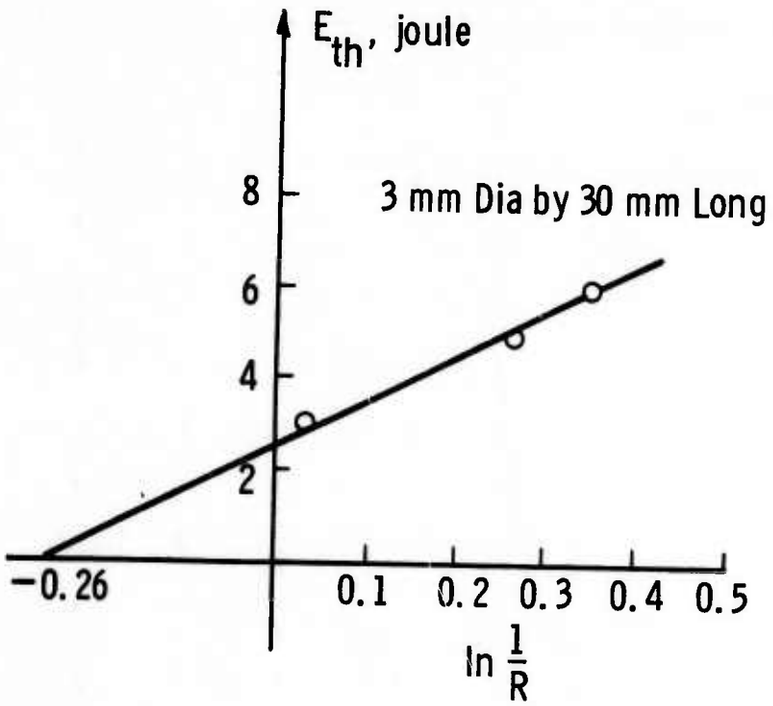

Fig. 22

Curve 594874-A

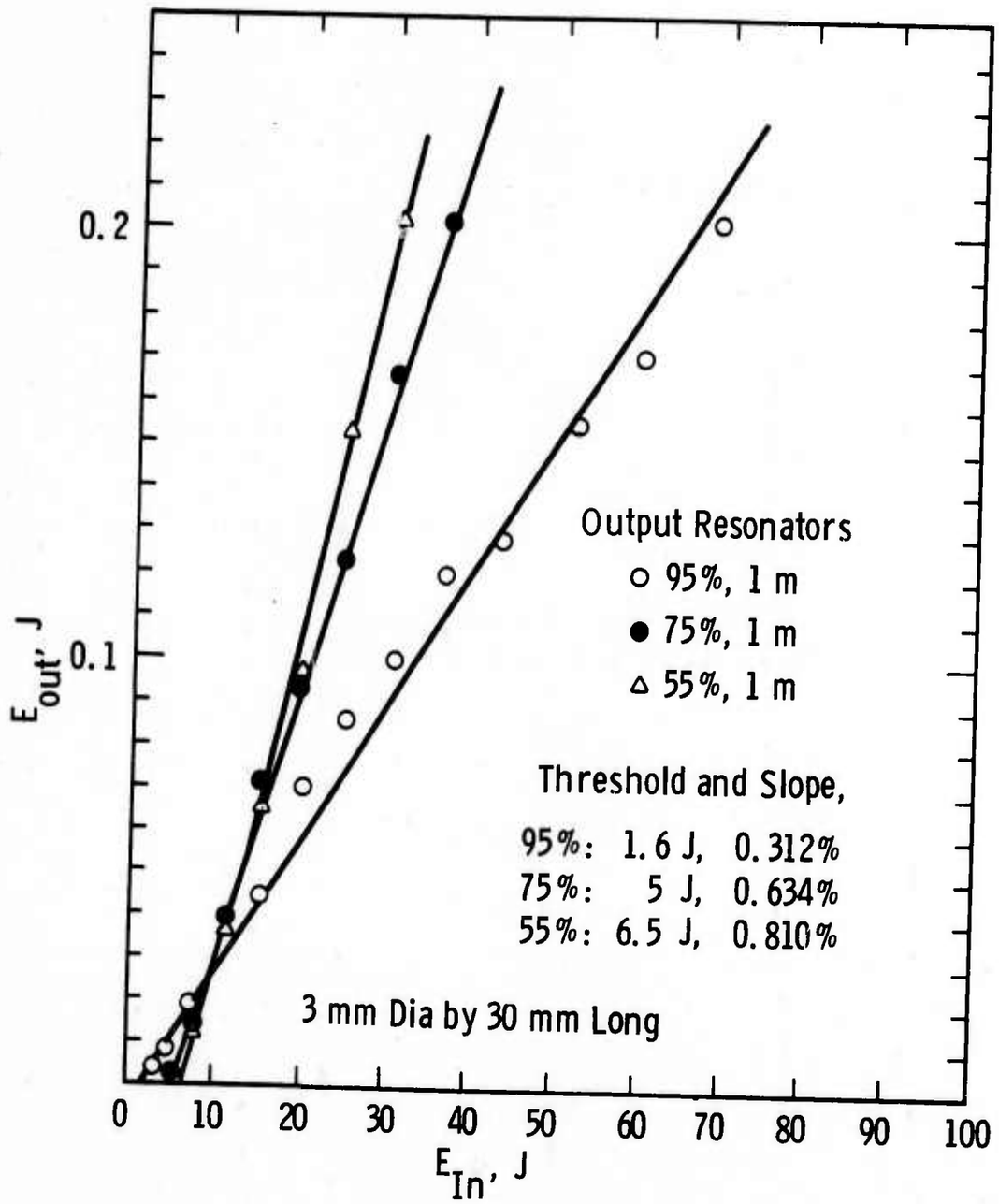

Fig. 23

Curve 594877-A

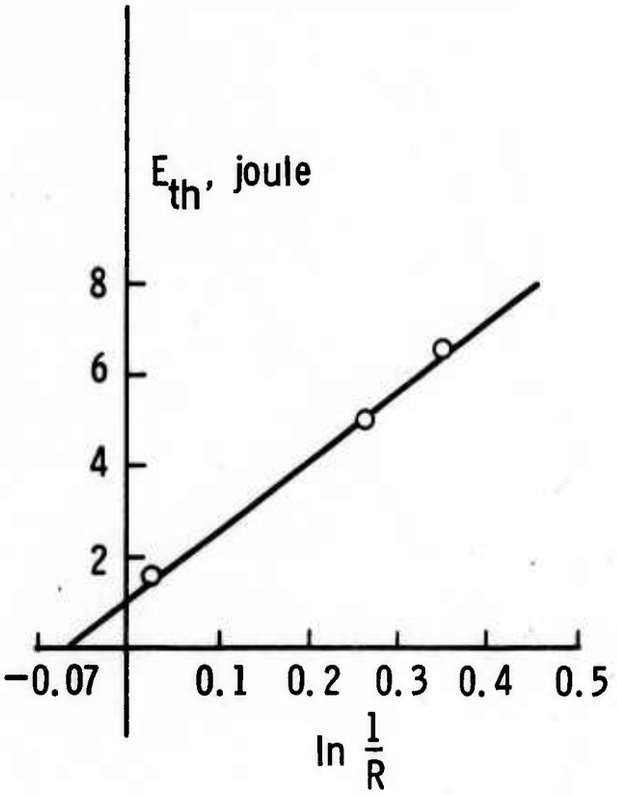

Fig. 24

0.31 to 1.20% depending on output coupling. That CaYSOAP crystals contain higher scattering losses than YAG is not surprising at this stage in our investigations. Continued refinement of crystal growth procedure should reduce this difference.

We must also recall, when comparing YAG and CaYSOAP, the large difference in spontaneous emission linewidth, and hence gain, between the materials. The fluorescence linewidth of the most prominent line (2.06μ) in CaYSOAP is 200 to 250Å wide while the most predominant line (2.098) for YAG is only about 25Å at 77°K (Ref. 2 and Section 3.2). On this basis we would expect a YAG laser to have a threshold perhaps ten times less than that of CaYSOAP which is about what we observe. On the other hand, the total energy contents of the $^5I_7 \rightarrow {}^5I_8$ transitions in both materials are similar, so that under similar pumping conditions, both materials should have comparable slope efficiencies. Our data show that the slope efficiency of CaYSOAP was between a factor of two to five lower than that of YAG, and this fact is no doubt related to the high losses in the CaYSOAP crystals. As crystal quality improves so also should the efficiency of CaYSOAP lasers

3.3.2.2 Q-Switched Measurements

Q-switch tests were attempted on two CaYSOAP:Er,Tm,Ho rods, #18-203380 and 108-203381, and on the two sensitized YAG-Ho rods, Linde #17284 C and 1720Y.

We used our liquid nitrogen-cooled test head for Q-switch testing in a conventional manner. A Glan prism and lithium niobate Pockel's cell were used for Q-switching, and these were placed between

the laser rod and the high reflectivity rear mirror. Apart from providing the necessary Q-switch data, the apparatus demonstrated the feasibility of using a lithium niobate Pockels' cell and Glan prism for Q-switching two micron laser radiation.

The Pockel's cell and Glan prism were anti-reflection coated for 1.06μ radiation since they are normally used to test Nd lasers. Neither the CaYSOAP or YAG laser rods were anti-reflection coated. We expect that the presence of so many reflecting surfaces in the resonator cavity probably results in significant cavity loss, and hold-off problems for high gain materials like YAG.* We plan to obtain a properly coated Pockel's cell and prism for future tests. Some CaYSOAP rods were birefringent to light propagating along the rod axis, thus signifying that the c direction and rod axis did not coincide. For this reason we used a He-Ne laser to obtain proper alignment of the rod and Q-switch.

During Q-switching of CaYSOAP we used resonators having a one meter radius of curvature and reflectivities of 99.9% and 55%. Maximum energy output was obtained with a delay of 770 μsec between the initiation of the lamp pulse and the switching of the Pockel's cell. A calibrated TRG thermopile served as radiation detector. We also obtained long pulse data from this same system by testing the rods with no voltage applied to the Pockel's cell.

---

*We did see indications of a hold-off problem with YAG but we were unable to obtain data due to the damage problem discussed at the end of this section.

Table 3 is a summary of the test results for rod #18-203380. Note that there was no evidence of saturation of the output during Q-switching up to the maximum energy that we put into the lamp. We observed that the difference in slope efficiency between Q-switched and long pulse operation varied from rod to rod (see also Table 4). A similar phenomena was observed for FAP:Nd and YAG:Nd lasers.[7]

Q-switch and long pulse data for CaYSOAP crystal #108-203381 is given in Table 4. While Q-switching was obtained from this rod, the results were more erratic than for rod #18-203380. Energy output varied from shot to shot and occasionally double pulses were obtained. Replacement of the Glan prism initially gave substantial improvements in the test results, but these could not be reproduced later. However, Table 4 again shows that saturation effects are absent up to the maximum Q-switched output, 50 mj.

Tables 3 and 4 indicate that the thicker rod, #108-203381 gave higher output energies for the same input energy than did the thinner rod. In all probability this again is a manifestation of the fact that rod #18-203380 is optically thin and is not strongly absorbing the pump radiation.

We pointed out in Table 2 that the dynamic loss coefficients for the YAG rods were much lower than for any of the CaYSOAP rods. Despite this fact, both YAG rods showed repeated damage each time a Q-switch measurement was attempted, and therefore no Q-switch data could be obtained for YAG. The test conditions for the YAG rods were identical with those described above for CaYSOAP rod. We note that

Table 3. Q-Switch and Long Pulse Operation of CaYSOAP:Er,Tm,Ho (#18-203380)

E_{in} (joules)	Long Pulse E_{out} (m-joule)	Q-Switched E_{out} (m-joule)
123	28	21
111	13	12
100	7	9
89	3	3

Table 4. Q-Switch and Long Pulse Operation of CaYSOAP:Er,Tm,Ho (#108-203381)

E_{in} (joules)	Long Pulse E_{out} (m-joule)	Q-Switched E_{out} (m-joule)
135	91	50
123	62	42
111	35	17
100	8	5.4

all the tests performed so far were made with either one or both external resonators curved. Similar measurements with flat resonators are planned which perhaps will prove less likely to damage YAG. CaYSOAP rods were Q-switched many times with no evidence for damage to the crystals.

3.3.2.3 CW Measurements

We attempted to obtain CW action from CaYSOAP rod #18-203380 at liquid nitrogen temperature, but were not successful with input powers up to 360 W. The CW threshold of the material evidently exceeds the power capabilities of our present system design.

We were, however, able to obtain CW operation when testing the two YAG rods, and these data are presented in Fig. 25. (Again, resonators have one meter curvature.) The output energy curve for 95% reflectivity and threshold for 99.9% reflectivity are indicated on the figure for rod #17284C. The slope efficiency for the rod is only 0.3%, a fact we attribute to the lack of anti-reflection coating on the rod ends and to the low color temperature of the lamp (50 W into an 800 W DXV lamp). The lamp was chosen because its filament matched the rod length.

The output energy of rod #1720Y with end coatings (0.4% transmission at the output end) is also shown in the figure. The threshold obtained was 15 W, and the output was 0.23 W with 70 W input to the lamp.

This same crystal was tested with external resonators (no A.R. coating) after the original end coatings were removed. The lowest threshold for this rod, 42 W, was obtained with 95% output reflectivity,

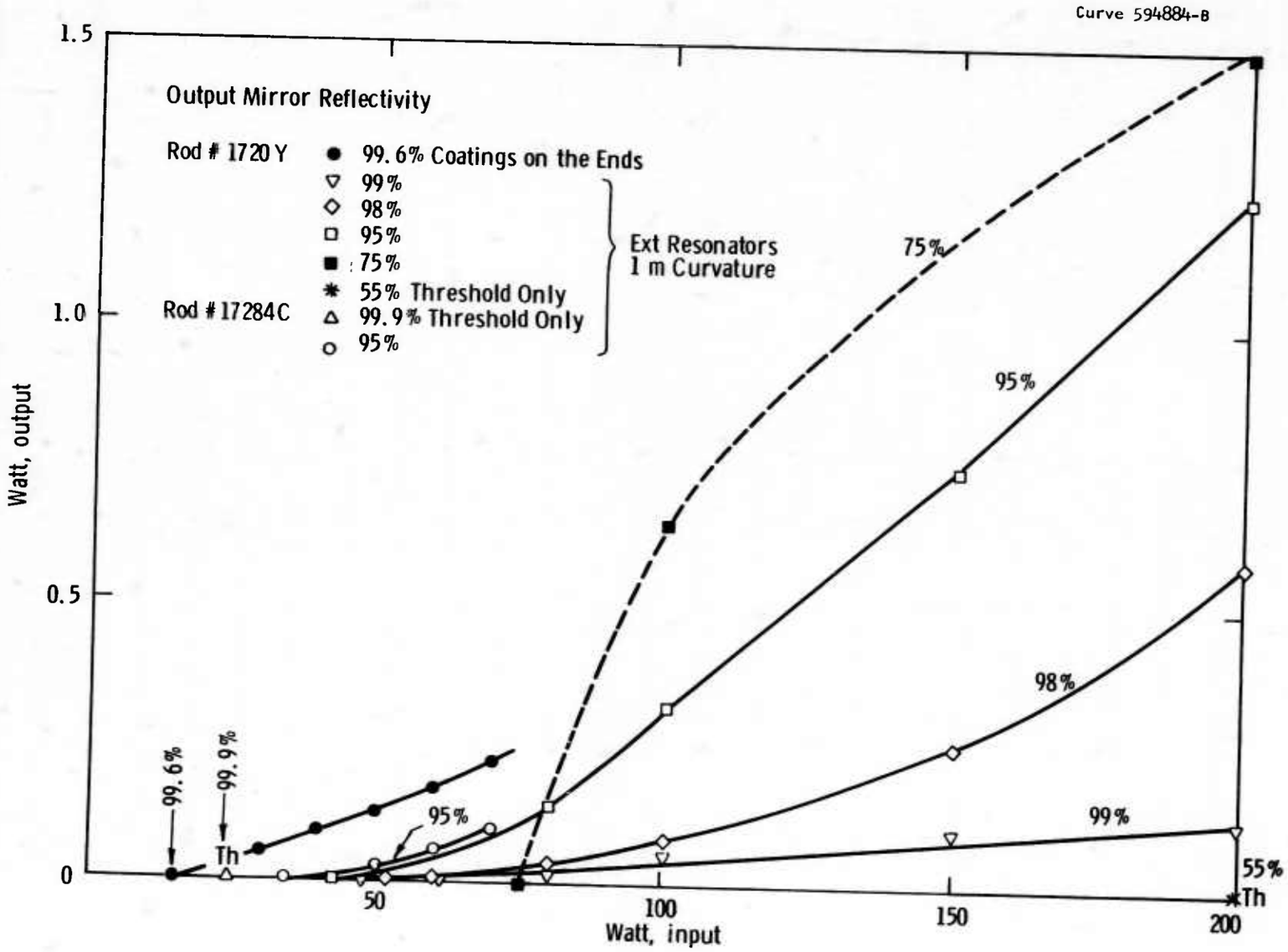
Curve 594884-B
1.5
1.0
0.5
0
Watt, output
Output Mirror Reflectivity
Rod # 1720 Y
99.6% Coatings on the Ends
99%
98%
95%
75%
Ext Resonators
1 m Curvature
55% Threshold Only
Rod # 17284C
99.9% Threshold Only
95%
75%
95%
98%
99%
99.6%
99.9%
95%
Th
55%
Th
50
100
150
200
Watt, input

Fig. 25

while thresholds with 99% and 98% reflectivities were higher. We think the causes for this inconsistency are a combination of a) loss of vacuum in the dewar over a period of time -- most likely by diffusion of the He into the dewar, and b) the high summer humidity. These cause freezing of the dewar, making testing difficult. Despite these problems, measurements were completed and the results are displayed in Fig. 25. The highest output power that was reproducibly measured was 1.5 W with a 75% output reflectivity and 200 W input. The highest slope efficiency measured was about 2.5%.

We mention for completeness that lasing was observed at 200 W input energy with 55% output reflectivity. No more detailed measurements were made. The above tests will be repeated as soon as the YAG rod is anti-reflection coated.

Presently seventy watts is about the maximum input power we can sustain for any reasonable length of time when the test system is cooled by gravity feeding the liquid nitrogen. Above that power so much gas is created around the rod that the system no longer functions. To alleviate this condition we introduced a miniature electric pump into the system to circulate the liquid nitrogen coolant. With this pump the power input range is extended to at least 360 W for short times. High power levels still cannot be maintained for long times due to the limited ability of the heat exchanger in our system to keep liquid nitrogen at a temperature below its boiling point. Once boiling begins the efficiency of the pump is drastically reduced. Therefore, to maintain high power levels for long durations, we would have to increase the heat exchanger size; this is not planned at the moment.

3.3.2.4 Frequency Doubling Experiments

The output wavelength of CaYSOAP:Er,Tm,Ho laser rod #18-203380 was measured by frequency doubling the laser output with a proustite (Ag_3AsS_3) crystal. The wavelength of the second harmonic was 1.03 μ, and we observed that the different modes lased over a 15Å wavelength range. This corresponds to a fundamental wavelength of 2.06 μ, with a wavelength variation of 30Å.

The frequency doubling measurements were performed using an existing 0.5 in. JACO spectrometer equipped with a 595 line grating blazed at 0.75 μ. Suitable optics were used in front of the spectrometer to focus the laser beam onto the spectrometer slits and simultaneously to fill the grating. The laser rod was mounted in the liquid N_2 cooled laser head. External resonators were used at both ends of the laser cavity. Detection was by means of an S-1 photomultiplier.

The use of external resonators made possible frequency doubling measurements with the proustite either in or outside the laser cavity. In the latter case the beam was focused on the second harmonic generating crystal. The internal geometry appeared to give the highest conversion efficiency, but in both cases the SHG energy was too low to measure by the calorimeter used. The SHG spike intensities correlated well with the spiking of the laser only in the internal SHG configuration; in the external SHG mode, polarization hopping and mode hopping in the laser rod and mode mixing in the SHG crystal reduced the correlation. The orientation dependence of the SHG phase-matching process was also measured. Insertion of the proustite crystal into the laser cavity

caused only a small increase in the laser threshold, implying that the losses due to the proustite are much smaller than the combined rod and cavity losses.

These measurements are described in greater detail in Appendix II.

3.3.3 FAP:Ho,Cr

Four more FAP:Ho,Cr rods have been tested since the last report. All tests were in the long pulse mode. Three of the rods failed to lase up to an energy input of 120 joules to the flashlamp. The fourth rod which was 18 mm long x 4.4 mm diameter lased with a 20 joule threshold when operated with a 99% reflectivity output resonator and a 31 joule threshold with a 95% output resonator. No threshold could be obtained up to 120 joules input with a 75% output mirror. With the 95% output resonator the slope efficiency of the FAP:Ho,Cr rod was 0.02%. These data are too sparse to draw any conclusions. We are now in the process of growing more FAP:Ho,Cr crystals to determine if the low efficiency for the rod described is typical.

4. DISCUSSION

4.1 CONCLUSIONS

Our efforts during this second six month contract period have centered primarily on phases 2 and 3 of the program. This work has consisted of initial crystal growth refinement studies, physical property measurements, and active laser testing of both CaYSOAP:Er, Tm, Ho and FAP:Ho, Cr. Some comparative laser tests of rare earth sensitized YAG:Ho were also made.

Crystal growth studies of CaYSOAP indicate that the major defects in these crystals are second phase inclusions formed during growth and a fine dispersion of second phase particles which develop in crystals held a high temperature for prolonged periods. We have inferred from these results that the stoichiometric and maximum melting compositions of CaYSOAP do not coincide and are therefore examining crystals pulled from non-stoichiometric melts in hopes of eliminating second phases from the crystals. Pull rates of less than 2 mm/hr and rotation rates around 80 rpm produce the best FAP:Ho, Cr crystals. The effective distribution coefficients of Cr and Ho in FAP crystals grown under these conditions are 0.25 and 0.34, respectively.

We have obtained from the literature, or measured, those physical properties of CaYSOAP:Er, Tm, Ho and FAP:Ho, Cr most likely to influence laser system design. These include refractive index, thermal expansion coefficient, thermal conductivity, heat capacity, lattice parameter, and hardness. We note that the thermal expansion coefficients

(5.7×10^{-6} °K^{-1}, [0001] and 7.1×10^{-6}, [$10\bar{1}0$]) and thermal conductivity (0.016 watt cm^{-1} °K^{-1} at 10°C) of CaYSOAP are both slightly lower than those of FAP.

Emission measurements on CaYSOAP:Er, Tm, Ho laser rods indicate no evidence for Er^{+3} or Tm^{+3} fluorescence, hence transfer to Ho^{+3} of the energy absorbed by these ions during pumping is probably complete. The intensity of c-axis fluorescence at 2.06μ is about 30% greater than the a-axis fluorescence in this material. All laser rods grown so far have been oriented in the c-direction. The transmission spectra of FAP:Ho, Cr crystals are essentially the same at room temperature and 77°K; both indicate the large overlap in transition energies for the Cr and Ho ions. This latter fact accounts for the good transfer yields from Cr to Ho. Spin resonance data tentatively identify the site symmetry of Cr in FAP as a distorted tetrahedron suggesting Cr substitution for P in the lattice.

We have begun active laser testing of CaYSOAP:Er, Tm, Ho and FAP:Ho, Cr and also performed some comparative tests on YAG:Ho. While the FAP:Ho, Cr results are too few in number to assess yet, our initial studies of CaYSOAP indicate that this material is especially promising for Q-switched applications. We have obtained 50 mj of Q-switched output from a rod of composition $CaY_{2.25}Er_{1.5}Tm_{.15}Ho_{.1}(S.O_4)_3O$ with no saturation evident up to the 135 joule input used. No damage to the rod was found during Q-switching while a YAG:Ho rod tested under identical conditions repeatedly damaged each time Q-switching was attempted. Long pulse tests of triply doped CaYSOAP indicate that these early

crystals contain 10 to 15% losses per cm which probably accounts for the fact that slope efficiency in CaYSOAP was somewhat less than in YAG (slope efficiencies for CaYSOAP ranged 0.1 to 0.6% and YAG 0.3 to 1.2%). The thresholds of CaYSOAP crystals varied between 28 and 70 joules at 77°K depending on reflectivity compared to 3-6 joules for YAG in agreement with the fact that the fluorescence linewidth for YAG is about ten times smaller than that of CaYSOAP. The larger fluorescence linewidth of CaYSOAP indicates that the energy storage per Q-switched pulse should be much higher than for YAG.

By means of frequency doubling the output of a CaYSOAP:Er, Tm, Ho laser with a proustite crystal we determined that the laser wavelength was 2.06μ ± 20 A°.

4.2 FUTURE PLANS

Final crystal growth refinement and intensive laser testing of FAP:Ho, Cr and triply-doped CaYSOAP will be emphasized in the final third of this program. Based on the laser data obtained we will assess the apatite hosts relative to other state-of-the-art Ho lasers such as YAG.

Specifically, our goal is to reduce scattering losses in CaYSOAP crystals by choice of proper melt composition. The growth conditions for FAP are fairly well characterized and large boules suitable for extensive laser testing will be grown.

Spectroscopic measurements will include decay and transfer times. These measurements have been held in abeyance pending modifications of the experimental equipment to eliminate spurious signals.

Attempts will be made to investigate more completely the nature of Cr in FAP. The problem of tailoring the dopant concentration to the rod thickness in CaYSOAP will also be considered.

Laser measurements will be refined. For example anti-reflection coatings suitable for 2μ operation will be applied to the laser rods and laser testing of both FAP and CaYSOAP in long pulse, Q-switch and CW modes will be completed.

REFERENCES

1. N.T. Melamed, R. Mazelsky, R.H. Hopkins, et al, Study of the Efficiency Improvement of Optically Pumped $Ca_5(PO_4)_3F$:Nd and $Ca_5(PO_4)_3F$:Ho, Cr, Technical Report AFML-TR-69-184, (1969).
2. R.H. Hopkins, N.T. Melamed, T. Henningsen and G.W. Roland, Rare-earth Doped Apatite Laser Materials, Technical Report AFAL-TR-70-103, (1970).
3. R.H. Hopkins, J. Crystal Growth, V6, p. 91, (1969).
4. R. Mazelsky, R.H. Hopkins, and W.E. Kramer, J. Crystal Growth, V3,4, p. 260, (1968).
5. R.H. Hopkins and W.E. Kramer, J. Electrochem Soc., V116, p. 637, (1969).
6. B. Cockayne, J. Crystal Growth, V3,4, p. 60, (1968).
7. R.H. Hopkins, K.B. Steinbruegge, and N.T. Melamed, CW and Q-switched Capabilities of Nd-doped Calcium Fluorophosphate, Technical Report AFAL-TR-69-239, (1969).
8. F. Knoop, C. Peters and W. Emerson, J. Nat. Bureau Standards, V23, p. 39, (1939).
9. L.F. Johnson, J.E. Geusic, and L.G. Van Uitert, Applied Phys. Letters, V8, p. 200 (1966).
10. E. Banks, M. Greenblatt, and B.R. McGarvey, J. Chem. Phys., V47, p. 3772 (1967).

11. R.C. Ohlmann, K.B. Steinbruegge and R. Mazelsky, Applied Optics, V7, p. 905 (1968).

12. J. Ito, Amer. Mineralogist, V53, 1968, p. 890.

13. B.D. Cullity, Elements of X-ray Diffraction, Addism-Wesley (Reading, Massachusetts) p. 87 (1959).

APPENDIX I

THERMAL PROPERTIES OF SYNTHETIC FLUORAPATITE CRYSTALS

R.H. Hopkins, D.H. Damon, P. Piotrowski,
M.S. Walker and J.H. Uphoff

(to be published in Journal of Applied Physics)

ABSTRACT

Measurements of the heat capacity, thermal expansion and thermal conductivity on synthetic crystals of undoped and neodymium-doped fluorapatite are reported. Fitting the low temperature specific heat data to a Debye model yields a Debye temperature of 550°K. At 25°C the thermal expansion coefficients are 10.0×10^{-6} $°K^{-1}$ and 9.4×10^{-6} $°K^{-1}$, respectively, along the [0001] and [$10\bar{1}0$] directions. The thermal expansion measurements yield a Debye temperature of 500°K. A typical value of the thermal conductivity is 0.020 watt cm^{-1} $°K^{-1}$ at room temperature. The thermal conductivity is only feebly temperature dependent and, similar to the thermal expansion coefficient, shows very little crystallographic anisotropy.

1. Introduction

Fluorapatite (FAP), one of a family of compounds which crystallize in the hexagonal space group $P6_3/m$, has the chemical formula $Ca_5(PO_4)_3F$ with 42 atoms per unit cell. Large single crystals of FAP, in which Ca has been partially replaced by Nd, exhibit laser oscillations at 1.06μ with unusually low thresholds and high efficiencies.[1] The apparatus for growing FAP crystals by the Czochralski method has been described in detail by Mazelsky, et al.[2] and the pulled crystals have been fully characterized with respect to crystal chemistry,[3] macroscopic imperfections,[4] and dislocation structure[5,6] in a series of previous papers. The purpose of this paper is to complete the physical property characterization of fluorapatie by presenting experimental data pertaining to the heat capacity, thermal expansion and thermal conductivity of FAP single crystals.

All data presented here were measured on a' and c crystals, i.e., those grown parallel to the $[10\bar{1}0]$ and [0001] directions, respectively, of the hexagonal lattice.[6] The dislocation contents of these crystals are typically $10^5/cm^2$ for a' crystals and $10^3/cm^2$ for c crystals.[5,6] Undoped crystals have lattice dimensions $a = 9.3697 \pm 0.0004$ Å and $c = 6.8834 \pm .0008$ Å.[3]

2. Heat Capacity

The heat capacity of an undoped single crystal fluorapatite sample was measured at temperatures in the range 4°K to 110°K in a heat capacity calorimeter designed[7] for measurements in the temperature range of 2°K to 25°K. Experimental error for the calorimeter in the latter range as determined by measurements of the heat capacity of copper was ± 1% scatter about a ± 3% shift in the entire heat capacity curve which occurred from run to run. For the study of fluorapatite the same copper sample was used in a single calibration run to 110°K which showed a steady increase in systematic error starting at 30°K and reaching a maximum of about ± 10% at 110°K. The total heat capacity of the calibrating copper sample was comparable throughout the entire range to that of the 3.55 gram fluorapatite sample.

The uncorrected results of the heat capacity measurements on an undoped a' crystal of FAP are shown in Figs. 1 and 2. The nearly linear variation of C/T with T^2 shown in Fig. 1, characteristic of an ideal solid at low temperatures, is somewhat deceptive since a tail of lower slope below 5°K must be expected for the curve to pass through the origin. At higher temperatures a leveling off of the heat capacity to a constant value may be indicated as shown in Fig. 2. Measurements at the higher temperatures are apparently subject to systematic errors due to uncontrollable changes in experimental conditions, as indicated by the dashed line in the figure which was drawn through heat capacities measured in a second run. Although the error can be quite large, it is believed that the curve is qualitatively correct. The data from about 25°K on down

are known to be accurate as indicated above. By fitting the results measured between 7° and 20°K to a Debye law, a value of 550°K was obtained for the Debye temperature.

3. Thermal Expansion

The thermal expansion coefficient of Nd-doped fluorapatite was calculated from the change in length of cylindrical FAP:2%Nd rods[1] as a function of temperature between 100 and 470°K. Measurements were carried out by means of a quartz tube dilatometer on 0.6 cm diameter by 2.54 cm long single crystals of each orientation. All tests were done in air.

Figures 3 and 4 show the thermal expansion (change in length per unit length) during both heating and cooling cycles for the c and a' orientations, respectively. Some hysteresis is obvious in both figures; the reason for this effect is not clear. For reference the thermal expansion coefficient was calculated at room temperature by taking the slope of the curve in each figure at 25°C. This is indicated by the dotted line passing through the point of zero expansion and 25°C.

The values of thermal expansion coefficients calculated in this way are 10.0×10^{-6} °K^{-1} in the c direction and 9.4×10^{-6} °K^{-1} along the a' direction. These values are probably valid over the temperature interval 240 to 330°K. Outside this interval thermal expansion varies non-linearly with temperature. A striking feature of Figs. 3 and 4 is the small difference in thermal expansion coefficient between c and a' orientations. (As discussed in the following section, the thermal conductivity also shows very little crystallographic anisotropy.) This

property is a decided advantage: it implies that FAP:Nd laser rods will expand almost isotropically when optically pumped. Hence the tendency toward crystal fracture due to anisotropic straining should be minimized.

Assuming thermal expansion is approximately proportional to the total vibrational energy of a crystal, the above thermal expansion data was fit to a Debye model. A good fit was obtained for a Debye temperature of about 500° which agrees well with the value obtained from heat capacity data.

4. Thermal Conductivity

The thermal conductivity of both undoped and neodymium-doped fluorapatite has been measured between 90 and 400°K. The apparatus used to measure the thermal conductivity has been described in detail elsewhere.[8] In brief, a stationary heat flow method was used with copper-constantan thermocouples for thermometers. The ends of the samples were ultrasonically tinned and soldered between the sink and the sample heater. This heater was guarded to reduce radiative heat losses. Corrections were made for the remaining heat losses which for the samples of fluorapatite were less than 12% of the total heat generated. In order to check the accuracy of the corrections for radiative heat loss one of the samples was first measured with the sample heater in the correct position within the guard heater. The length of the sample was then reduced by 1.1 mm with the result that the sample heater was dropped out of the guard by this amount. Using the same radiation correction a difference of 5% was found between the two thermal conductivities. A small correction

(∿ 1% of the total thermal resistance) was made for the thermal resistivity of the solder layers. The accuracy of these measurements is, therefore, estimated to be 3 to 4%. All of the samples were roughly of the same size, being no smaller than 4 x 4 x 11 mm.

The thermal conductivity of four samples cut from Czochralski ingots was measured. Two of the samples were cut so that the heat flow was along the c axis and two with the heat flow along the a' axis. Two of the samples were doped with 2% neodymium substituted for calcium and two were undoped. The measured values of the thermal conductivity are plotted against absolute temperature, T, in Fig. 5.

We note the following:

(1) The values of the thermal conductivity are very small considering that these samples are single crystals of a high melting temperature material composed of light atoms;

(2) The thermal conductivity is insensitive to temperature;

(3) The crystallographic anisotropy in the thermal conductivity is small;

(4) For heat flow along the a' direction the addition of the Nd causes a small but apparently significant decrease in the thermal conductivity; for heat flow along the c direction the Nd doping seems to have no significant effect;

(5) For all samples there is a slight increase in the thermal conductivity with increasing temperature between 300 and 400°K.

The last listed observation is a result of radiative transport of heat through the sample. It is not easy to account for the radiation

through the sample which depends on the infrared optical properties of the material. If we assume that the photon mean free path is equal to the length of the sample and that the static dielectric constant ($\sim$ 10 for fluorapatite[3]) may be used to characterize the radiative transmission of heat, then one finds that the thermal conductivity would be augmented by a radiative contribution of 0.019 and 0.007 watt $cm^{-1}\ °K^{-1}$ at 400 and 300°K respectively. This is an upper limit for the radiative contribution. In order to obtain a rough estimate of the importance of this contribution, one of the samples was cut in half, soldered back together and remeasured. The measured thermal conductivities were found to be smaller by .0008 and .003 watt $cm^{-1}\ °K^{-1}$ at 300 and 390°K respectively. The change observed at 390°K $\sim$ 15% is certainly significant. Assuming that this decrease in K may be attributed to halving the photon mean free path then the radiative contribution to the thermal conductivity might be about .006 watt $cm^{-1}\ °K^{-1}$ at 390°K.

If we subtract a radiation contribution of this size from the measured values, then the resulting thermal conductivity becomes a more rapidly varying function of temperature. However, the decrease of K with increasing T is still not as great as would be predicted by a T^{-1} law expected for good crystals at high temperature. In fact, considering the Debye temperature (> 500°K), one would expect the thermal conductivity to vary somewhat faster than T^{-1} in the temperature range 100 to 400°K.

It may be objected that our crude estimate of the radiative contribution does not constitute a measurement of this quantity which, in view of our calculated upper limit, may be considerably larger. However, the results shown in Fig. 5 cannot be fit to an equation of

the form $K = aT^{-1} + bT^3$ for any choice of constants a and b. Moreover, the assumption of a radiative contribution of the order of our calculated upper limit would reduce the true lattice thermal conductivity at 400°K to a value typical of a glass. Even without considering a radiative contribution the measured values of the thermal conductivity are much smaller than would be expected for perfect crystals of fluorapatite.

A number of theoretical calculations and semi-empirical analyses have been made to relate the lattice thermal conductivity, K_L, of solids to other properties such as the Debye temperature and the thermal expansion. Most of these schemes agree with each other and with the experimental results within a factor of 2 to 6. Keyes[9] semi-empirical relationship, $K_L = BT_m^{3/2} \rho^{2/3} A^{-7/6}$, relating lattice thermal conductivity to melting point, T_m, density, ρ, and mean atomic weight, A, accounts for the thermal conductivity of 34 elements and compounds within a factor 2 if one value of B is chosen for solids with ionic bonding and another value for covalent bonding. Using 1920°K for T_m, ρ = 3.19 g cm^{-3}, and 25.2 for the mean atomic weight, Keyes' relationship predicts that the lattice thermal conductivity of fluorapatite should be 0.2 watt cm^{-1} $°K^{-1}$ at 300°K if the bonding is primarily ionic (for covalent bonding the value would be 1.6 watt cm^{-1} $°K^{-1}$). Part of the explanation of this order of magnitude discrepancy between the experimental results and this calculation is probably to be found in the vibrational properties of the PO_4^{-3} radicals. In order to fit the data for $CaCO_3$ into his scheme, Keyes found it necessary to treat the CO_3^{-2} radical as a single large atom, ignoring its internal degrees of freedom. If the same assumption is made for the PO_4^{-3} radical in fluorapatite the predicted value

of K_L at 300°K becomes 0.074 watt cm^{-1} $°K^{-1}$. In other words, the present experimental results force one to assume that many of the vibrational modes have very small group velocities and thus carry very little heat. Such a conclusion is certainly not surprising for a material with such a large unit cell.

This effect may help explain why the values of the thermal conductivity are so small, but cannot explain the temperature dependence. Theory suggests that the insensitivity of the thermal conductivity to temperature change can only be explained by strong phonon scattering by defects.[10] The present results show that the substitution of 2% Nd for Ca in this material causes only a slight decrease in the thermal conductivity. The dislocation densities in these samples, viz., 10^3 to 10^5 lines/cm^2 are much too small to affect the thermal conductivity. Thus, we can rule out phonon scattering by chemical impurities and dislocations. It is known that fluorapatite crystals may contain fluoride vacancy concentrations as large as 10 at %.[3] Previous work in this laboratory[8] has shown that vacancies may be extremely effective phonon scatterers even at high temperatures. We have not attempted a quantitative analysis of these results because of:

(1) the uncertainty in the radiative contribution to the heat transport;

(2) the difficulties in the analysis of thermal conductivity in a temperature range where neither high or low temperature approximations are valid.

A complete account must await further elucidation of the phonon scattering mechanisms through measurements of the thermal conductivity at very low temperatures.

5. Conclusions

The principal features of both the low temperature heat capacity and the thermal expansion coefficients of fluorapatite can be fit to a Debye model with a Debye temperature between 500 and 550°K. Measured values of the thermal conductivity are small and only feebly dependent on temperature. These measurements suggest that only a fraction of the vibrational modes carry the heat and that there may be significant phonon scattering by vacancies.

We believe the low thermal conductivity is a principal factor in limiting to low values the CW power output of laser rods fabricated from Nd-doped fluorapatite crystals. The inability of laser rods to dissipate heat results in thermal distortion and refractive index variations within the rods. This in turn increases the laser beam divergence and, at sufficiently high power inputs, also causes catastrophic fracture of the laser rod.

Acknowledgment

The authors thank Mr. C. Hager and Mr. J. Valentich for carrying out the thermal expansion measurements. They are indebted to Dr. R. W. Warren for help in analyzing the expansion measurements. This investigation was partially supported by the Air Force Avionics Laboratory under Contract F33615-65-1550.

References

1. R. C. Ohlmann, K. B. Steinbruegge and R. Mazelsky, Appl. Optics, 7, 5 (1968).
2. R. Mazelsky, R. C. Ohlmann and K. B. Steinbruegge, J. Electrochem. Soc., 115, 68 (1968).
3. R. Mazelsky, R. H. Hopkins and W. E. Kramer, J. Crystal Growth, 3,4, 260 (1968).
4. R. H. Hopkins and W. E. Kramer, J. Electrochem. Soc., 116, 637 (1969).
5. G. M. McManus, R. H. Hopkins, and W. J. Takei, J. Appl. Phys., 40, 180 (1969).
6. R. H. Hopkins, J. Crystal Growth, 6, 91 (1969).
7. M. S. Walker, unpublished research, Westinghouse Research Laboratories.
8. D. H. Damon, J. Appl. Phys., 37, 3181 (1966).
9. R. W. Keyes, Phys. Rev., 115, 564 (1959).
10. P. G. Klemens, Phys. Rev., 119, 507 (1960).

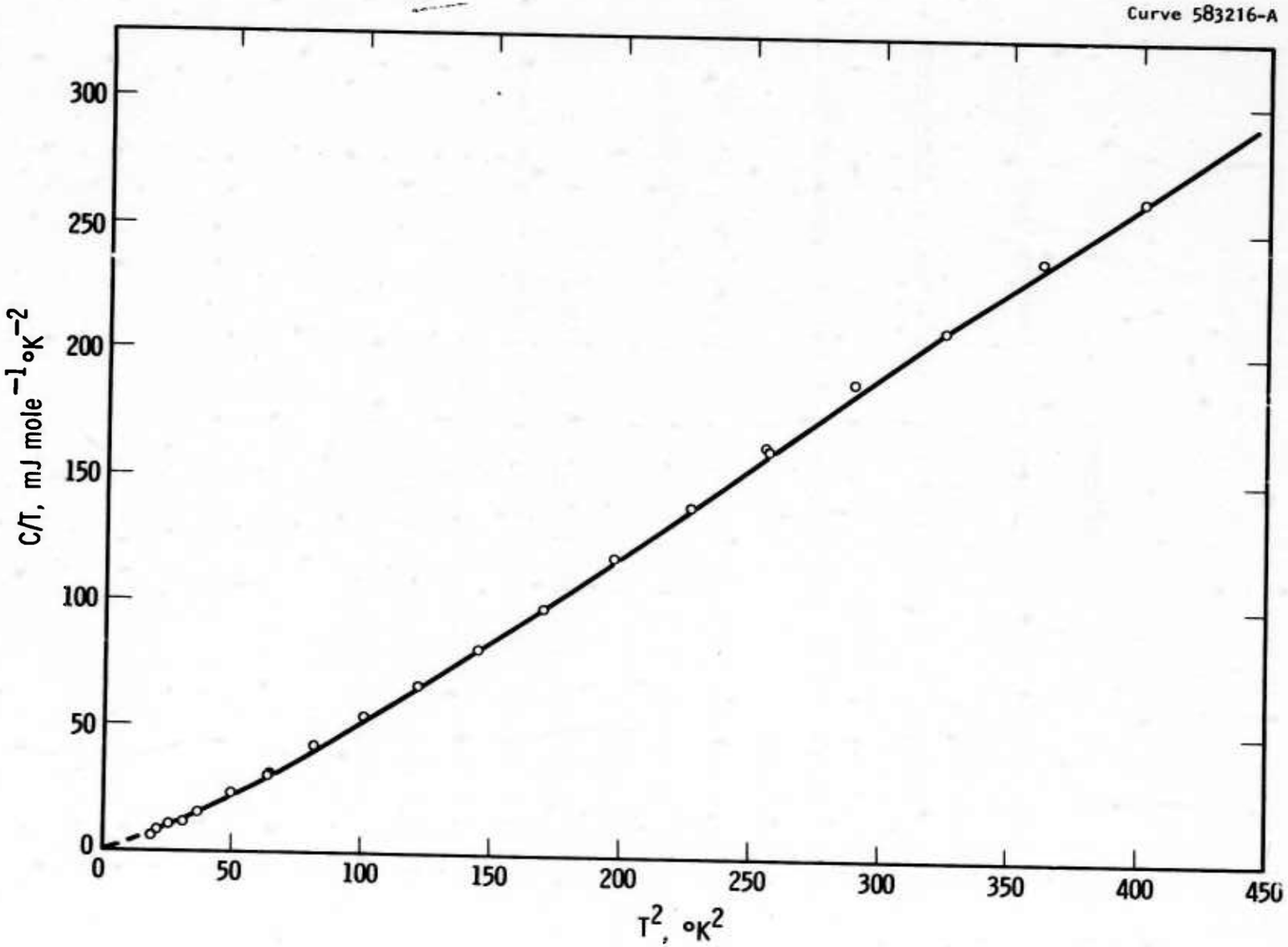
Curve 583216-A
C/T, mJ mole^{-1} °K^{-2}
T^2, °K^2
0
50
100
150
200
250
300
350
400
450

Fig. 1

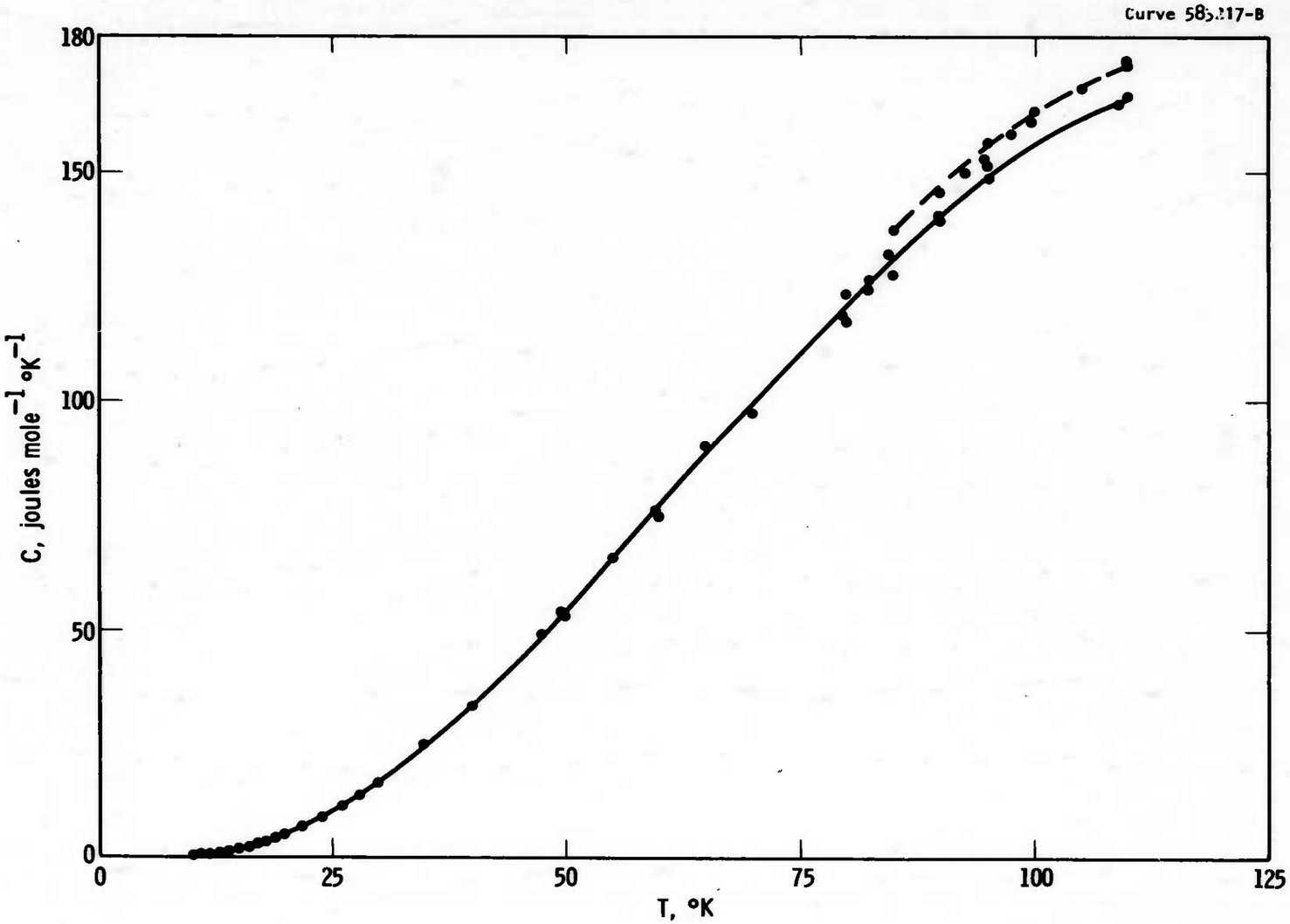
Curve 585-17-B
180
150
100
50
0
0
25
50
75
100
125
C, joules mole^{-1} °K^{-1}
T, °K

Fig. 2

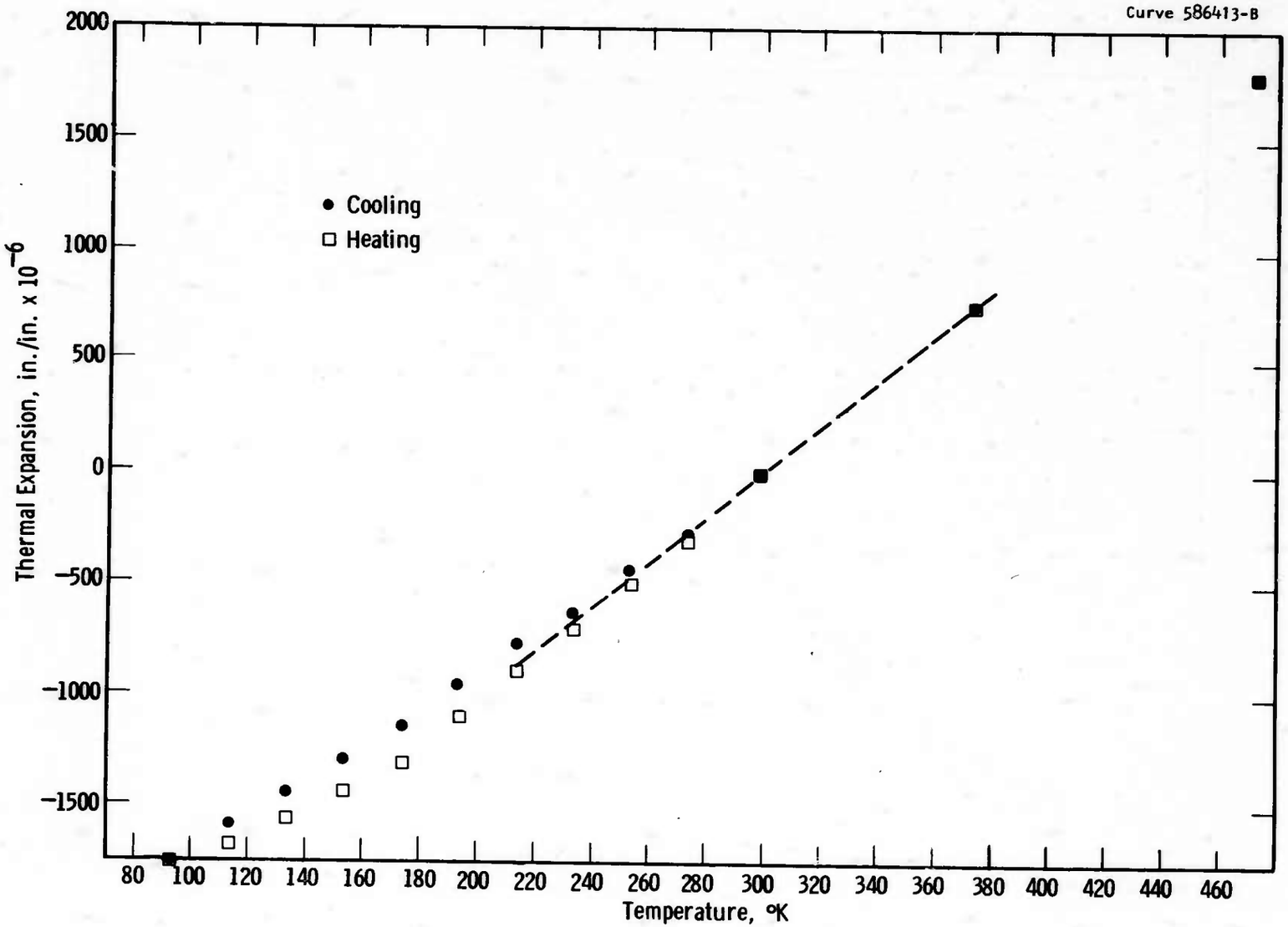
Curve 586413-B
2000
1500
1000
500
0
−500
−1000
−1500
Thermal Expansion, in./in. x 10⁻⁶
● Cooling
□ Heating
80 100 120 140 160 180 200 220 240 260 280 300 320 340 360 380 400 420 440 460
Temperature, °K

Fig. 3

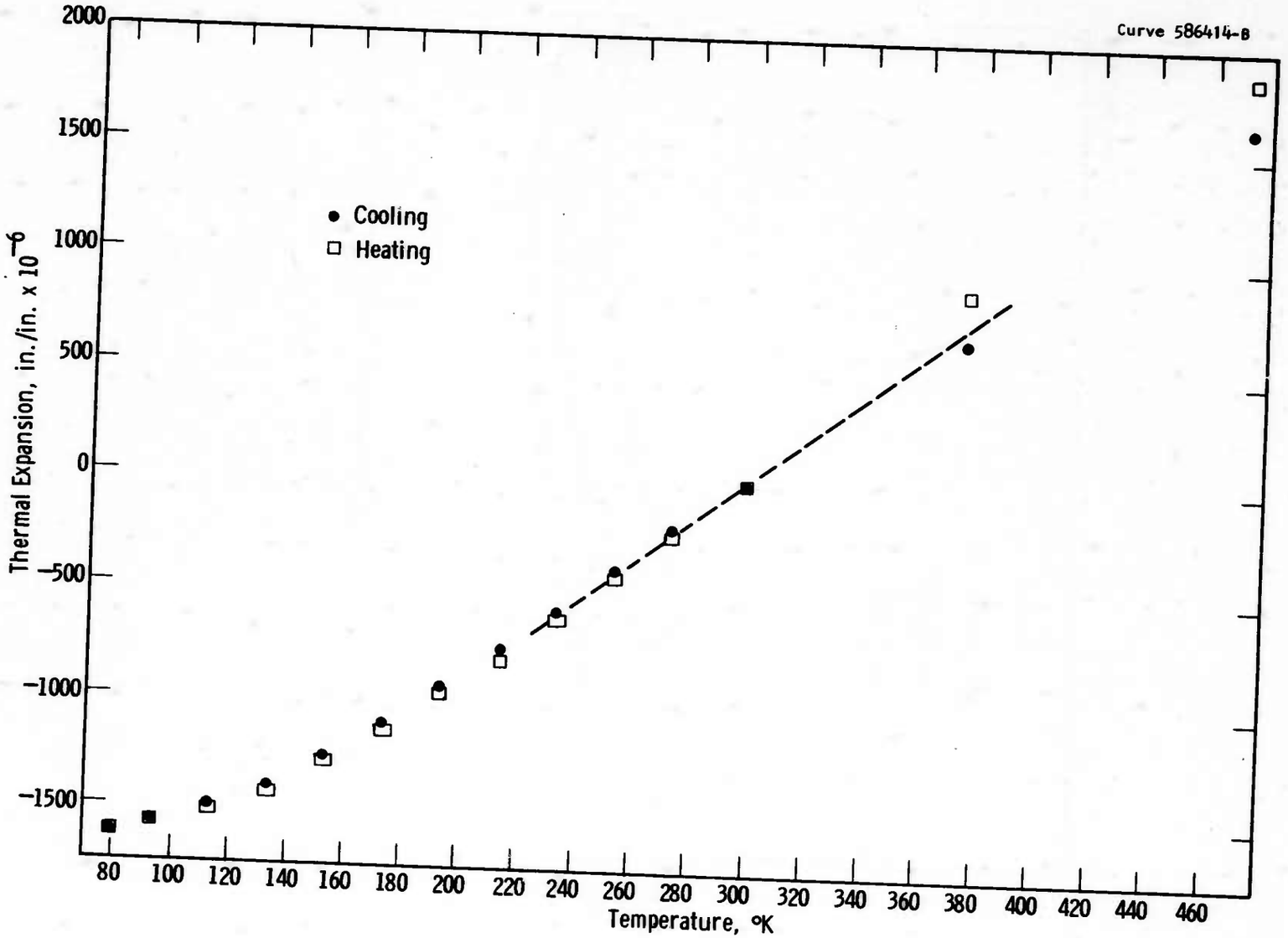
Curve 586414-B
Cooling
Heating
Thermal Expansion, in./in. x 10⁻⁶
2000
1500
1000
500
0
−500
−1000
−1500
80
100
120
140
160
180
200
220
240
260
280
300
320
340
360
380
400
420
440
460
Temperature, °K

Fig. 4

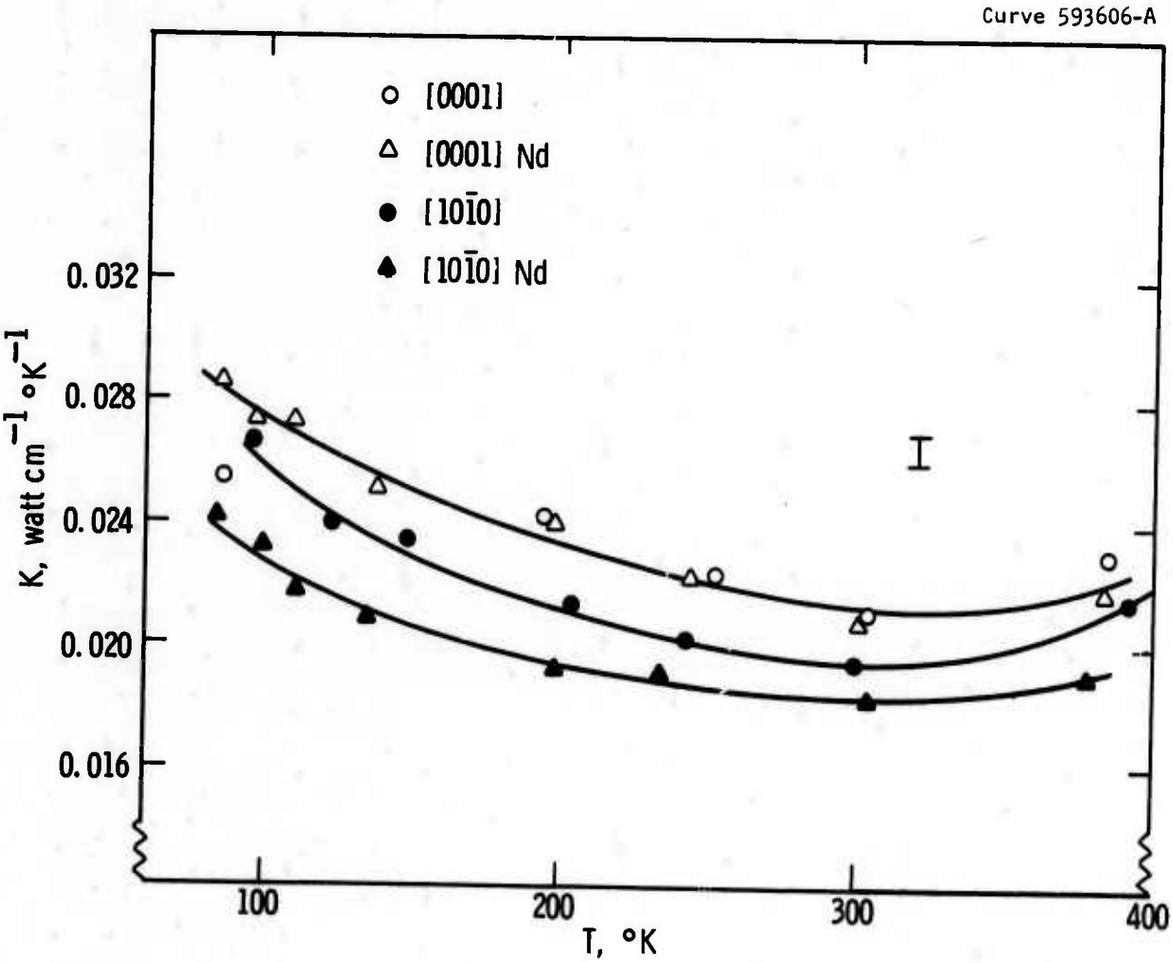
Curve 593606-A
[0001]
[0001] Nd
[10$\bar{1}$0]
[10$\bar{1}$0] Nd
0.032
0.028
0.024
0.020
0.016
K, watt cm^{-1} °K^{-1}
100
200
300
400
T, °K

Fig. 5

APPENDIX II

FREQUENCY DOUBLING OF 2.06μm Ho-DOPED APATITE LASER OUTPUT IN Ag_3AsS_3*

T. Henningsen, J. D. Feichtner, and N. T. Melamed

Westinghouse Research Laboratories
Pittsburgh, Pennsylvania 15235

(Submitted to IEEE J. Quantum Electronics)

ABSTRACT

Frequency doubling of the 2.06μm output of a Ho-doped CaY-silicate oxyapatite laser operating in the long-pulse mode has been observed in an experiment using single crystal Ag_3AsS_3 (proustite) as the nonlinear optical material. Phase-matched second harmonic generation was obtained at 30°53' with respect to the crystal axis. The experiment was performed in two different ways. In one case, a focusing geometry was used with the crystal outside the laser cavity; in the other, the nonlinear material was placed within the laser cavity. Conversion efficiencies were low (<<1%) due primarily to the low power densities used. The wavelength of the second harmonic radiation (1.03μm) is readily detected with conventional high-speed S-1 photomultipliers; this allows convenient room-temperature monitoring and measurement of 2 μm Apatite laser outputs with existing equipment.

*Work supported by the Air Force Avionics Laboratory, Wright-Patterson Air Force Base, Ohio under Contract F33615-70-C-1051.

1. INTRODUCTION

Although the technology of detectors for the near infrared region of the spectrum is advancing rapidly, detectors for the region beyond 1.1μ are in most cases, even when cooled, limited in speed and detectivity in comparison to photomultipliers. For this reason, and for convenience in measuring the laser output wavelength, we investigated frequency doubling of the 2μm output of a Ho:Apatite laser material currently under development.[1]

Proustite (Ag_3AsS_3)[2] was chosen as the nonlinear optical material. While not unique for this application, it is readily available in good optical quality, exhibits low losses at both fundamental and second harmonic frequencies, possesses reasonably high nonlinear optical coefficients, and does not require temperature phase matching. Other possible materials include lithium niobate[3] and barium sodium niobate.[4] Although they have suitable spectral regions of low absorption loss, both materials exhibit only moderate optical quality in their present state of development, and are susceptible to damage at high power densities. KD*P is too lossy at 2.06μm and its effective nonlinear optical coefficient is relatively small. Lithium iodate ($LiIo_3$) and pyrargyrite (Ag_3SbS_3) are other promising candidates, but were not immediately available.

2. EXPERIMENTAL PROCEDURES

The experimental apparatus is shown schematically in Fig. 1. The source of the coherent 2 μm radiation was a Ho-doped laser made from an apatite single crystal material which is currently under development called calcium yttrium silicate oxyapatite[1] (CaYSOAP). The laser rod was 25 mm long by 3 mm diameter, and was mounted in a specially designed horizontal liquid N_2 dewar not shown in the figure. Two special features of this dewar are: a) except for very short sections at each end, the rod is completely immersed in liquid N_2, thereby insuring uniform cooling and good thermal contact. Bubble formation is prevented by maintaining the N_2 several degrees below its boiling point, and b) the dewar does not contain windows at either end, and permits us to use external resonators at either or both ends of the laser cavity. This feature provides complete freedom to insert optical components into the laser cavity. The laser was pumped with a PEK Xe1-1.5 xenon flashlamp. Both the rod (with its dewar) and the flashlamp were mounted within a 9" i.d. spherical pump cavity.[5] The entire assembly was mounted on an optical bench to permit easy alignment with a spectrometer.

The proustite crystal used for frequency doubling was also grown in our laboratory. The finished crystal was 1.2 cm in diameter and 1.07 cm long. It was cut at an angle of 30°, 53' with respect to its crystallographic c-axis, this angle calculated on the basis of Type

I phase matching $(0 + 0 \rightarrow e)$[6] using the refractive index of Hulme.[2] The crystal was gimbal mounted to permit alignment.

Two optical arrangements were used for second harmonic generation. In the first, shown in Fig. 1, the proustite crystal was mounted externally to the laser cavity. Ninety-five per cent and 75% reflectivity dielectric resonators with 1m radii of curvature were used for the laser cavity. A 16 cm focal length lens focused the 2μm laser beam into the crystal. Such a focal length lens corresponds to harmonic generation under weak focusing conditions. The second harmonic generated output (plus the transmitted fundamental) was focused on the slit of the monochromator by means of a second lens chosen to match the numerical aperture of the monochrometer. The monochromator was a 0.5m JACO equipped with a 595 line/mm grating which gave a linear dispersion of 32.9 Å/mm in first order. The dispersed frequency doubled radiation was detected with an RCA 8647 S1 photomultiplier terminated with a 100 ohm resistor. The phototube output was fed directly into a 555 Tektronix dual-beam oscilloscope. The laser oscillations were monitored at the high reflectivity end of the laser cavity with an InAs detector terminated by a 3.3 ohm load. The output of this detector was displayed on the second beam of the oscilloscope.

The second optical arrangement was similar to the first except that the proustite crystal was mounted inside the optical cavity, and the 16 cm focal length lens was omitted. The output coupling resonator, which had a 75% reflectivity in the external harmonic generation arrangement was changed to a 99.9% resonator with a 1m curvature.

3. EXPERIMENTAL RESULTS

Figure 2 shows a typical result of second harmonic generation with the crystal outside the laser cavity operating in the weakly focused configuration. The upper trace shows the output of the Ho laser as detected at the rear output mirror. The 2μm energy incident on the proustite was 50 mj, and consisted of a 600μsec long train of pulses. Individual pulses were less than 5μsec in half-width; our ability to measure pulse widths was limited by the response time of the InAs detector. The diameter of the focal spot within the proustite crystal was estimated to be 0.1 cm. We estimate the average power density to have been about 0.01 Mw/cm^2 over the 600μsec pulse, although the spiking of the laser output no doubt resulted in considerably higher instantaneous power densities (up to 0.5 Mw/cm^2). No damage was observed in the Ag_3AsS_3 crystal after many repeated measurements at these levels.

The lower portion of Fig. 2 shows the second harmonic radiation as detected by the S1 photomultiplier after having passed through the monochromator. A filter chosen to transmit the second harmonic but to block the fundamental radiation was placed between the proustite and the monochromator in order to eliminate chances for spurious photomultiplier signals. The generated second harmonic radiation was detected by the photomultiplier at a monochromator setting of 1.030 μm and with a slit width corresponding to 1.5 Å resolution. By varying the monochrometer

wavelength setting and slit openings, we conclude that the frequency of oscillations of the SOAP:Ho laser is 2.060 μm within an approximately 8Å bandwidth.

Although it is not immediately obvious in Fig. 2, there is good temporal correlation between the occurrence of the fundamental spikes and their second harmonic counterparts. However, the amplitudes of the frequency doubled spikes do not correlate well with the amplitudes of the corresponding spikes in the fundamental. This is a well-known consequence of mode-hopping, the change in the polarization of the laser output from spike to spike, and of the correlations between modes of a multi-mode spike induced by the nonlinear process.[7] This situation is improved by placing the harmonic generating crystal inside the laser cavity.

Figure 3 shows the results obtained with the proustite within the optical cavity of the laser. The data was obtained with the SOAP:Ho laser operating only slightly above threshold. The insertion of the proustite crystal into the laser cavity did not measurably increase the threshold of the 2μm laser despite the fact that the proustite faces were not AR coated. From this we conclude that the losses in the proustite are significantly less than the losses in the laser rod. The latter are approximately 10% per cm.

A greatly improved correlation between the amplitudes of the fundamental and frequency doubled spikes is seen in Fig. 3. The improvement results from the fact that, within the laser cavity, the birefringence of the nonlinear harmonic generating crystal creates excessive

walk-off for modes which are polarized so as to be extraordinary rays. The tendency, therefore, is to clamp the laser oscillations to a single polarization. In addition, because no focusing is used, the mode density in the nonlinear material is not as high as in the case where the crystal was external to the cavity and focusing was used. Mode correlation effects are thereby less pronounced.

The correlation between the amplitudes of the fundamental and frequency doubled spikes is sufficiently good for the internally mounted proustite that it was possible to obtain a direct confirmation of the quadratic dependence of the frequency doubled amplitude on the amplitude of the fundamental. This was done by measuring the amplitudes of the spikes in a series of photographs similar to Fig. 3, obtained under varying conditions of pump powers. The results are shown in Fig. 4. Except for the slight discrepancy at very low power levels, a linear relationship is obtained when the amplitude of the second harmonic output is plotted against the square of the peak of the fundamental. The small deviation at the low energy end is due to the fact that the half width of the spikes of the fundamental frequency are somewhat broader at very low energies than they are at intermediate and high energies; the peak response of the slower InAs detector is different for these pulses. The scatter in the data is not unexpected and is partly due to the difficulty in accurately determining the peaks of the spikes from the photographs. Despite these errors, a reasonably good quadratic dependence is obtained.

Finally, in Fig. 5, we plot the angular dependence of the second harmonic amplitude for the weakly focused configuration with the

Proustite external to the cavity. The conditions were those previously described for the external configuration. The full width at half-maximum of the phase matched region is seen to be $\Delta\theta_m = 0.56°$. A theoretical value[8] for this angular variation based on a focused TEM_{oo} gaussian beam is 0.022°. The discrepancy is due mainly to the multimode character of the laser output, and not to the Ag_3AsS_3 crystal quality. Evidence for this comes from experiments on frequency doubling of a CO_2 laser output in Ag_3AsS_3 using the same boule. The latter yielded an angular tuning response much closer to the theoretical value.

4. ACKNOWLEDGEMENTS

We wish to thank Dr. Richard Hopkins for growing the CaYSOAP:Ho laser crystal, Dr. G. W. Roland for growing the Proustite crystal, and Mr. A. Mego and Mr. V. Toth for their expert assistance in these experiments.

REFERENCES

1. R. H. Hopkins et al, in preparation; see also R. C. Ohlmann, K. B. Steinbruegge, and R. Mazelsky, Applied Optics 7, 905 (1968) for a related apatite laser.
2. K. F. Hulme, O. Jones, P. H. Davies and M. V. Hobden, "Synthetic Proustite (Ag_3AsS_3): A New Crystal for Optical Mixing," App. Phys. Lett. 10, 133 (1967).
3. G. E. Peterson, A. A. Ballman, P. V. Lenzo and P. M. Bridenbaugh, "Electro-optic Properties of Lithium Niobate," App. Phys. Lett. 5, 62 (1964).
4. J. E. Geusic, H. J. Levinstein, J. J. Rubin, S. Singh and L. G. Van Uitert, "The Nonlinear Optical Properties of $Ba_2NaNb_5O_{15}$," App. Phys. Lett. 11, 269 (1967).
5. C. H. Church and I. Liberman, "The Spherical Reflector for Use in Optical Pumping of Lasers," Appl. Optics 6, 1966 (1967).
6. J. E. Midwinter and J. Warner, "The Effects of Phase Matching Method and of Uniaxial Crystal Symmetry on the Polar Distribution of Second-Order Nonlinear Optical Polarization," Brit. J. Appl. Phys. 16, 1135 (1965).
7. See, for example, N. Bloembergen, "Some Theoretical Problems in Quantum Electronics," Proc. Symp. on Optical Masers, N.Y., 1963 (Polytechnic Press, Brooklyn, N.Y. 1963).

References (cont'd.)

8. F. R. Nash et al, "Optical Nonlinearities in $LiIo_3$," Jour. Appl. Phys. 40, 5201 (1969).

FIGURE CAPTIONS

Figure 1 - Apparatus used for second harmonic generation. The diagram shows the weak focussing configuration, with the proustite crystal external to the laser cavity. In the laternate mode of second harmonic generation, the proustite is placed between the laser rod and the 75% reflectivity mirror, and the 16 cm focal length lens is removed.

Figure 2 - The fundamental and frequency doubled signals obtained with the proustite external to the laser cavity, in a weakly focussed configuration. Upper trace: 2.06 μm output of SOAP:Ho, using InAs for detection; lower trace: 1.030 μm frequency doubled signal, as detected by an S1 photomultiplier after passing through a spectrometer. The time scale is 50 μsec/division.

Figure 3 - The fundamental and frequency doubled signals displayed as in Figure 2, but with the proustite crystal insider the laser cavity. Note the greatly improved correspondence between the fundamental and frequency doubled spikes.

Figure 4 - Second harmonic peak power as a function of the square of the fundamental peak power, showing the quadratic dependence of the second harmonic output on the fundamental peak power. Points were obtained from oscilloscope traces similar to that shown in Figure 3.

Figure 5 - Angular dependence of external phase-matched second harmonic generation of the SOAP:Ho laser in proustite. $\theta_m = 30° 22'$; rotation shown is in horizontal plane.

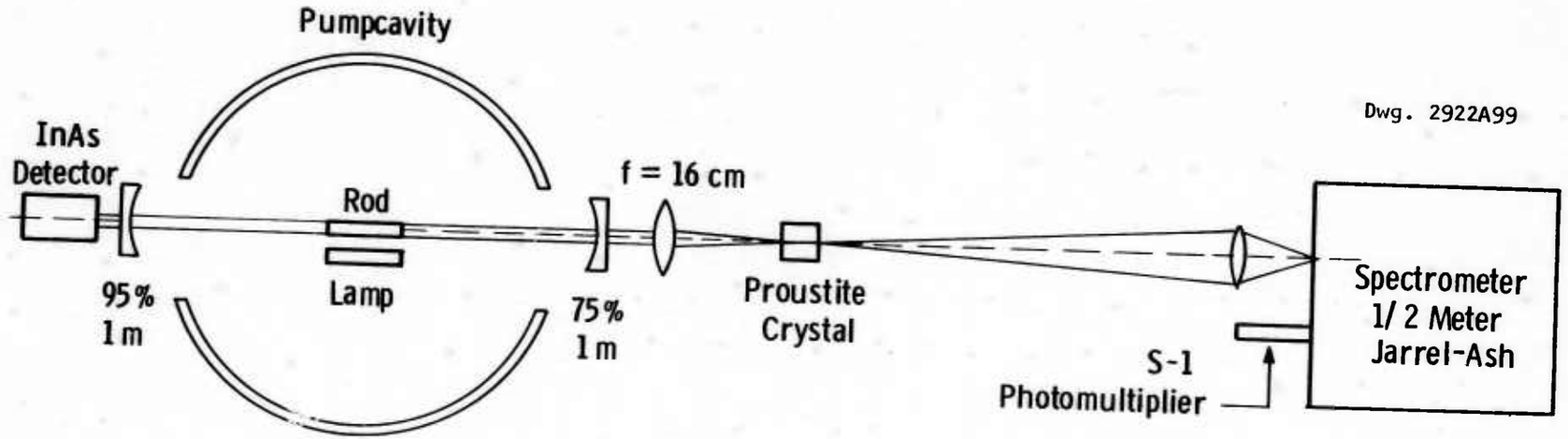
Pumpcavity
Dwg. 2922A99
InAs
Detector
Rod
f = 16 cm
95%
1 m
Lamp
75%
1 m
Proustite
Crystal
Spectrometer
1/2 Meter
Jarrel-Ash
S-1
Photomultiplier

Fig. 1

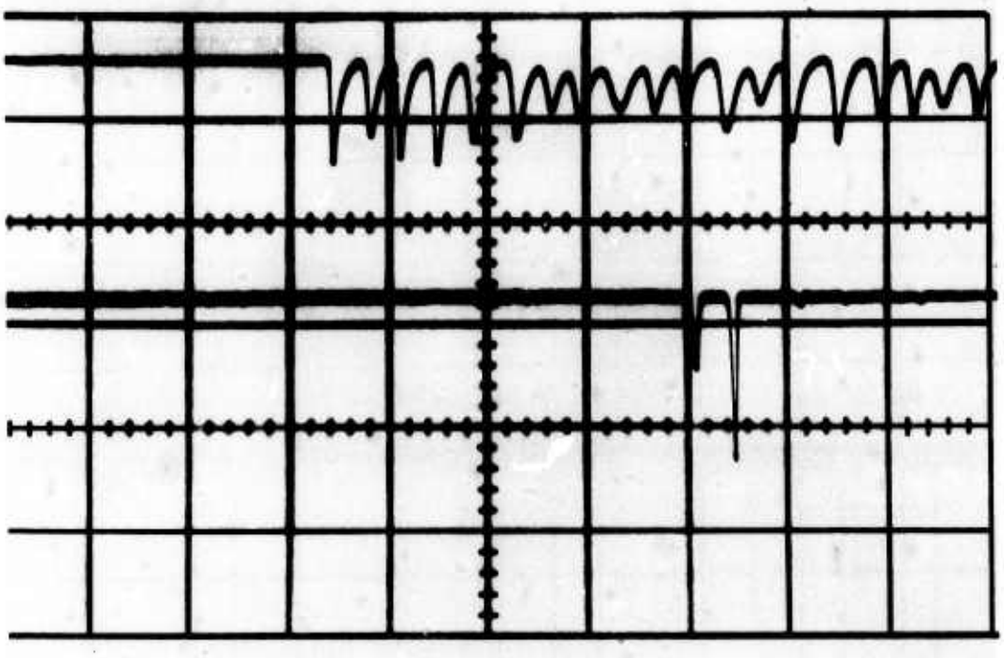

Figure 2

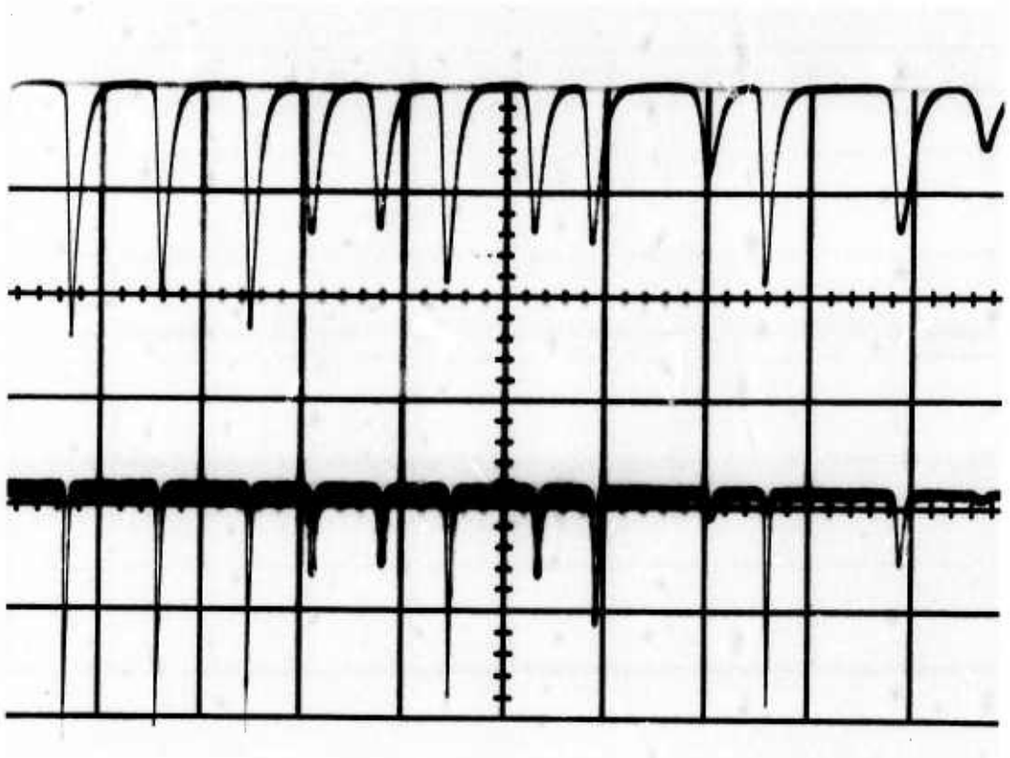

Figure 3

Curve 593756-A

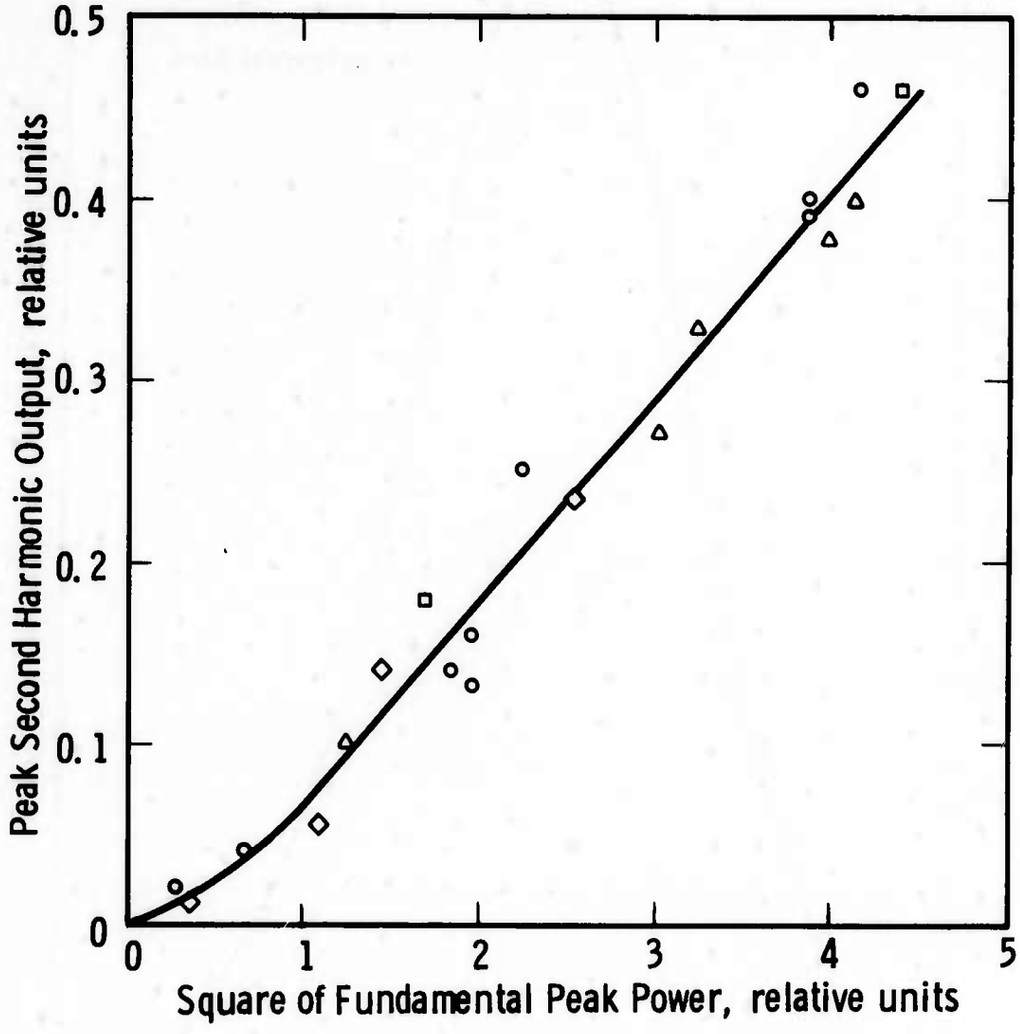

Fig. 4

Curve 593755-A

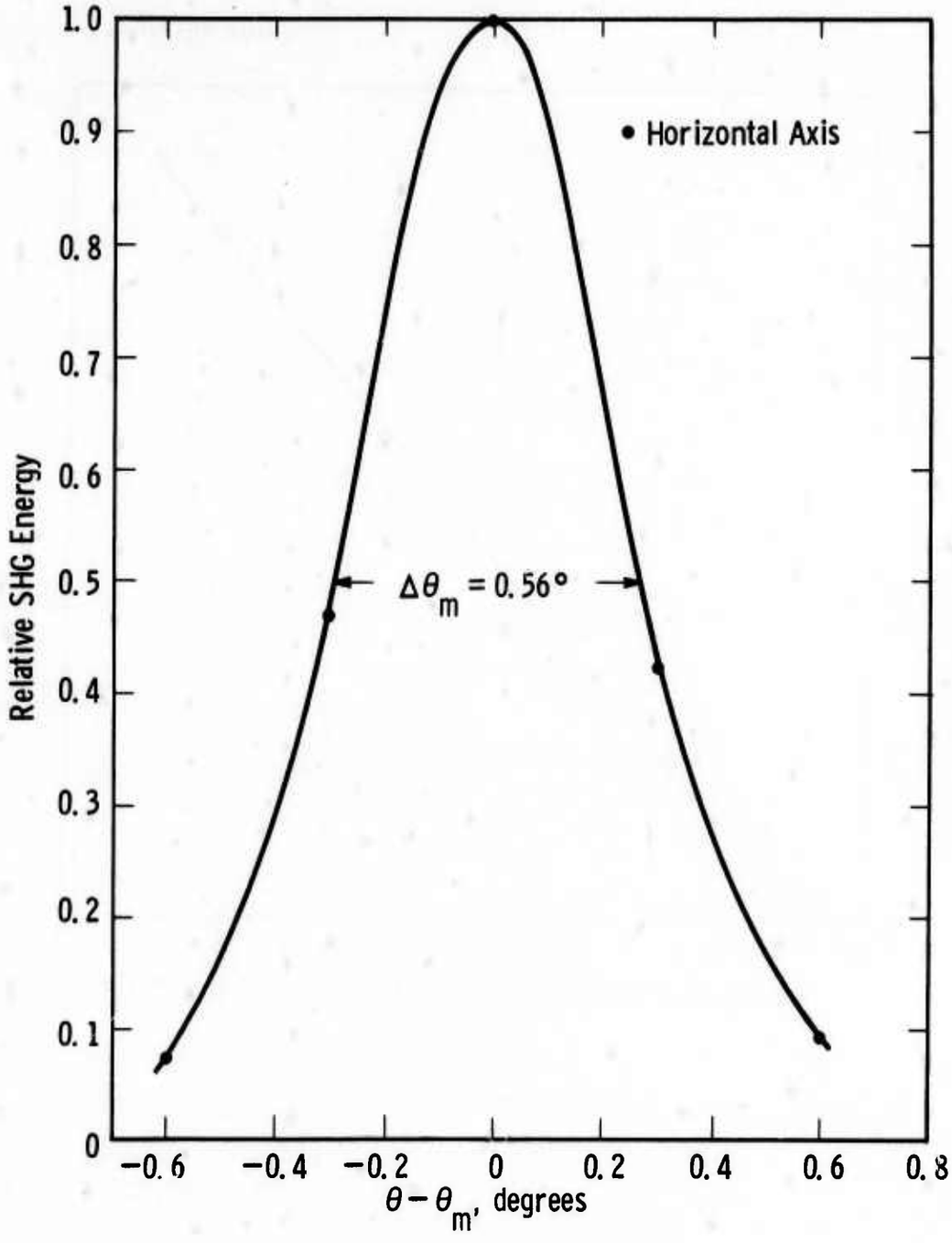

Fig. 5

Security Classification

DOCUMENT CONTROL DATA - R&D

(Security classification of title, body of abstract and indexing annotation must be entered when the overall report is classified)

1. ORIGINATING ACTIVITY *(Corporate author)*
Westinghouse Electric Corporation
Research Laboratories

2a. REPORT SECURITY CLASSIFICATION
UNCLASSIFIED

2b. GROUP

3. REPORT TITLE

RARE EARTH DOPED APATITE LASER MATERIALS

4. DESCRIPTIVE NOTES *(Type of report and inclusive dates)*
Semi-annual, 20 March 1970 to 19 September 1970

5. AUTHOR(S) *(Last name, first name, initial)*
Hopkins, Richard H. Roland, G.W.
Melamed, N.T.
Henningsen, T.H.

6. REPORT DATE	7a. TOTAL NO. OF PAGES	7b. NO. OF REFS
December 1970	100	13

8a. CONTRACT OR GRANT NO.	9a. ORIGINATOR'S REPORT NUMBER(S)
F33615-70-C-1051	70-6J8-REDAP-R2
b. PROJECT NO. ARPA Order 1467	
c.	9b. OTHER REPORT NO(S) *(Any other numbers that may be assigned this report)*
d.	

10. AVAILABILITY/LIMITATION NOTICES
This document is subject to special export controls and each transmittal to foreign governments or foreign nationals may be made only with prior approval of (TEL), WPAFB, Ohio

11. SUPPLEMENTARY NOTES	12. SPONSORING MILITARY ACTIVITY
	Air Force Avionics Laboratory Wright-Patterson AFB Ohio 45433

13. ABSTRACT

This second semi-annual report describes the current status of the second and third phases of a program to evaluate certain members of the apatite mineral family as hosts for the active laser ion holmium.

A systematic study of the effect of growth parameters in the quality of fluorapatite (FAP) crystals doped with holmium and chromium indicates that growth rates below 2 mm/hr and rotation rate of 80 rpm should be optimum for crystal growth. For these conditions the distribution coefficients of Ho and Cr in FAP are 0.34 and 0.24, respectively.

The physical properties of CaYSOAP have been measured and compiled. We have also tabulated these properties for FAP.

CaYSOAP exhibits a laser threshold of 30 to 60 joules at 77°K. Despite approximately 10% cm^{-1} scattering losses efficiencies of 0.61% have been obtained in long pulse tests from these crystals. An unsaturated Q-switch output of 50 mj with 135 j input to the lamp has been achieved for CaYSOAP.

DD FORM 1 JAN 64 1473

Security Classification

RM 35054

Security Classification

14. KEY WORDS	LINK A		LINK B		LINK C	
	ROLE	WT	ROLE	WT	ROLE	WT
laser two-micron apatite garnet holmium erbium thulium oscillator						

INSTRUCTIONS

1. ORIGINATING ACTIVITY: Enter the name and address of the contractor, subcontractor, grantee, Department of Defense activity or other organization *(corporate author)* issuing the report.

2a. REPORT SECURITY CLASSIFICATION: Enter the overall security classification of the report. Indicate whether "Restricted Data" is included. Marking is to be in accordance with appropriate security regulations.

2b. GROUP: Automatic downgrading is specified in DoD Directive 5200.10 and Armed Forces Industrial Manual. Enter the group number. Also, when applicable, show that optional markings have been used for Group 3 and Group 4 as authorized.

3. REPORT TITLE: Enter the complete report title in all capital letters. Titles in all cases should be unclassified. If a meaningful title cannot be selected without classification, show title classification in all capitals in parenthesis immediately following the title.

4. DESCRIPTIVE NOTES: If appropriate, enter the type of report, e.g., interim, progress, summary, annual, or final. Give the inclusive dates when a specific reporting period is covered.

5. AUTHOR(S): Enter the name(s) of author(s) as shown on or in the report. Enter last name, first name, middle initial. If military, show rank and branch of service. The name of the principal author is an absolute minimum requirement.

6. REPORT DATE: Enter the date of the report as day, month, year, or month, year. If more than one date appears on the report, use date of publication.

7a. TOTAL NUMBER OF PAGES: The total page count should follow normal pagination procedures, i.e., enter the number of pages containing information.

7b. NUMBER OF REFERENCES: Enter the total number of references cited in the report.

8a. CONTRACT OR GRANT NUMBER: If appropriate, enter the applicable number of the contract or grant under which the report was written.

8b, 8c, & 8d. PROJECT NUMBER: Enter the appropriate military department identification, such as project number, subproject number, system numbers, task number, etc.

9a. ORIGINATOR'S REPORT NUMBER(S): Enter the official report number by which the document will be identified and controlled by the originating activity. This number must be unique to this report.

9b. OTHER REPORT NUMBER(S): If the report has been assigned any other report numbers *(either by the originator or by the sponsor)*, also enter this number(s).

10. AVAILABILITY/LIMITATION NOTICES: Enter any limitations on further dissemination of the report, other than those imposed by security classification, using standard statements such as:

(1) "Qualified requesters may obtain copies of this report from DDC."

(2) "Foreign announcement and dissemination of this report by DDC is not authorized."

(3) "U. S. Government agencies may obtain copies of this report directly from DDC. Other qualified DDC users shall request through

_____."

(4) "U. S. military agencies may obtain copies of this report directly from DDC. Other qualified users shall request through

_____."

(5) "All distribution of this report is controlled. Qualified DDC users shall request through

_____."

If the report has been furnished to the Office of Technical Services, Department of Commerce, for sale to the public, indicate this fact and enter the price, if known.

11. SUPPLEMENTARY NOTES: Use for additional explanatory notes.

12. SPONSORING MILITARY ACTIVITY: Enter the name of the departmental project office or laboratory sponsoring *(paying for)* the research and development. Include address.

13. ABSTRACT: Enter an abstract giving a brief and factual summary of the document indicative of the report, even though it may also appear elsewhere in the body of the technical report. If additional space is required, a continuation sheet shall be attached.

It is highly desirable that the abstract of classified reports be unclassified. Each paragraph of the abstract shall end with an indication of the military security classification of the information in the paragraph, represented as *(TS)*, *(S)*, *(C)*, or *(U)*.

There is no limitation on the length of the abstract. However, the suggested length is from 150 to 225 words.

14. KEY WORDS: Key words are technically meaningful terms or short phrases that characterize a report and may be used as index entries for cataloging the report. Key words must be selected so that no security classification is required. Identifiers, such as equipment model designation, trade name, military project code name, geographic location, may be used as key words but will be followed by an indication of technical context. The assignment of links, rules, and weights is optional.

Security Classification

RM 35055